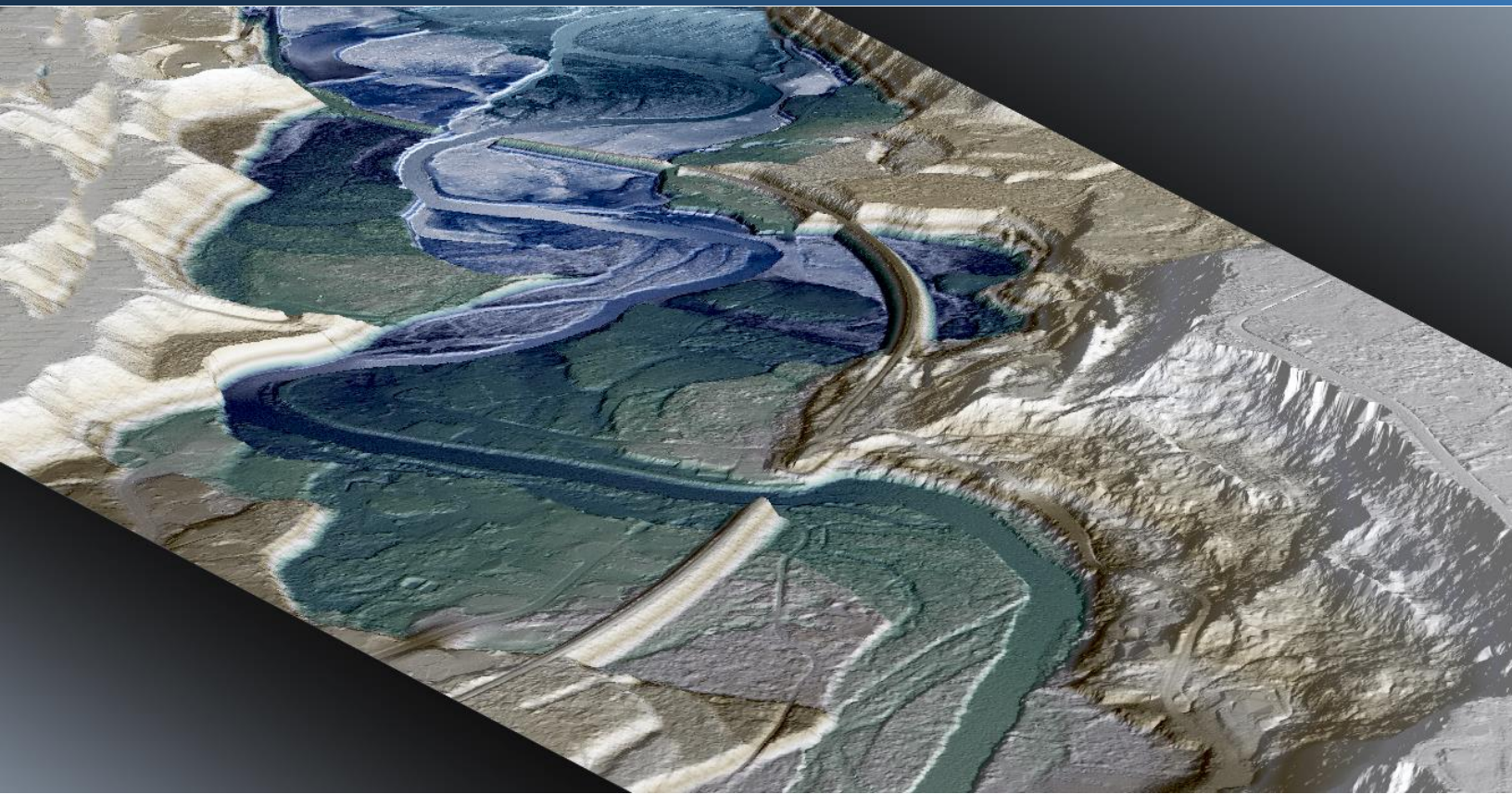


September 9, 2014



Cedar River Watershed & Floodplain, Lake Youngs Reservoir, & SCL/Tolt Reservoir Study Areas LiDAR

Technical Data Report – Delivery 2, revised October 22, 2014.



Andy Norton
1011 Western Avenue, Suite 500
Seattle, WA 98104
PH: 206-464-7427



QSI Corvallis Office
517 SW 2nd St., Suite 400
Corvallis, OR 97333
PH: 541-752-1204

TABLE OF CONTENTS

| | |
|--|----|
| INTRODUCTION | 1 |
| Deliverable Products | 3 |
| ACQUISITION | 5 |
| Planning..... | 5 |
| Ground Control..... | 6 |
| Monumentation | 6 |
| Ground Survey Points (GSP) | 7 |
| Airborne Survey..... | 10 |
| LiDAR..... | 10 |
| PROCESSING | 13 |
| LiDAR Data..... | 13 |
| RESULTS & DISCUSSION..... | 15 |
| LiDAR Density | 15 |
| LiDAR Accuracy Assessments | 19 |
| LiDAR Absolute Accuracy..... | 19 |
| LiDAR Vertical Relative Accuracy..... | 20 |
| CERTIFICATIONS | 22 |
| SELECTED IMAGES..... | 23 |
| GLOSSARY | 27 |
| APPENDIX A - ACCURACY CONTROLS | 28 |
| APPENDIX B – AOI ACCURACY STATISTICS | 29 |
| LiDAR First Return Point Density | 29 |
| LiDAR Ground Point Density | 30 |
| LiDAR Absolute Accuracy..... | 32 |
| LiDAR Relative Accuracy | 33 |

Cover Photo: A view looking northwest over two river crossings on the Cedar River Trail located in Wilderness Village, Washington. This image was created from the gridded LiDAR surface colored by elevation.

INTRODUCTION

This photo taken by QSI acquisition staff shows the mixed conifer landscape in the Cedar Watershed LiDAR site in the Cascade foothills of Washington.



In September 2013, WSI, a Quantum Spatial company (QSI), was contracted by the Puget Sound LiDAR Consortium (PSLC) to collect Light Detection and Ranging (LiDAR) data for three areas of interest (AOIs) in the greater Seattle, Washington area. The individual AOIs include the Cedar River Watershed and Floodplain, Lake Youngs Reservoir, and the SCL/Tolt Reservoir, herein all referred to as the Cedar Watershed LiDAR project (Figure 1). Data were collected to aid PSLC in assessing the topographic and geophysical properties of the study area.

On April 11, 2014, a section of the SCL/Tolt Reservoir AOI (Delivery 1) was delivered to the PSLC. This report accompanies the remaining section of the SCL/Tolt Reservoir AOI, the Cedar River Watershed AOI, and the Lake Youngs Reservoir AOI, all collectively referred to as Delivery 2. Included are Delivery 2 contract specifications, data acquisition procedures, processing methods, and analysis of the complete and final dataset including LiDAR accuracy and density. Acquisition dates and acreage are shown in Table 1, and a complete list of contracted deliverables provided to PSLC is shown in Table 2.

Table 1: Acquisition dates, acreage, and data types collected on the Cedar Watershed LiDAR site

| Project Site | Contracted Acres | Buffered Acres | Acquisition Dates | Data Type | Delivery Date |
|----------------------------|------------------|----------------|---|-----------|----------------|
| Cedar Watershed Delivery 1 | 108,769 | 111,737 | December 11, 12, and 16, 2013 and February 3, 5 – 6, 2014 | LiDAR | April 11, 2014 |

| Project Site | Contracted Acres | Buffered Acres | Acquisition Dates | Data Type | Delivery Date |
|-----------------------------------|------------------|----------------|---|-----------|-------------------|
| Cedar Watershed Delivery 2 | 198,881 | 206,896 | October 29 – 30, 2013, November 1, 3 - 4, 2013, December 3 – 5, 2013, February 5 – 7, 2014, June 22, 23, 30, 2014, and July 2, 5 - 8, 2014 | LiDAR | September 9, 2014 |



This photo taken by QSI acquisition staff shows a view of ground survey equipment set up for the Cedar Watershed project, with a view of Mt. Rainier in the background.

Deliverable Products

Table 2: Products delivered to PSLC for the Cedar Watershed LiDAR site

| Cedar Watershed LiDAR Products ¹ Projection: Washington State Plane North Horizontal Datum: NAD83 (HARN*) Vertical Datum: NAVD88 (GEOID03) Units: US Survey Feet | |
|---|---|
| Points | LAS v 1.2 <ul style="list-style-type: none"> • All Returns Comma Delimited ASCII Files <ul style="list-style-type: none"> • All Returns (*asc) • Ground Returns(*gnd) |
| Rasters | 3.0 Foot ESRI Grids <ul style="list-style-type: none"> • Bare Earth Model • Highest Hit Model 1.5 Foot GeoTiffs <ul style="list-style-type: none"> • Intensity Images |
| Vectors | Shapefiles (*.shp) <ul style="list-style-type: none"> • Site Boundary • LiDAR Tile Index • DEM Tile Index • Smooth Best Estimate Trajectory (SBETs) • Ground Survey Points & Monuments |

**The data were created in NAD83 (CORS96), but for GIS purposes are defined as NAD83 (HARN) as per PSLC specifications.*

¹ Additional contracted products will be provided to Seattle Public Utilities only, in a third and final delivery which includes a hydroflattened and hydroenforced bare earth model and hillshade, and a 3D hydrolines shapefile.

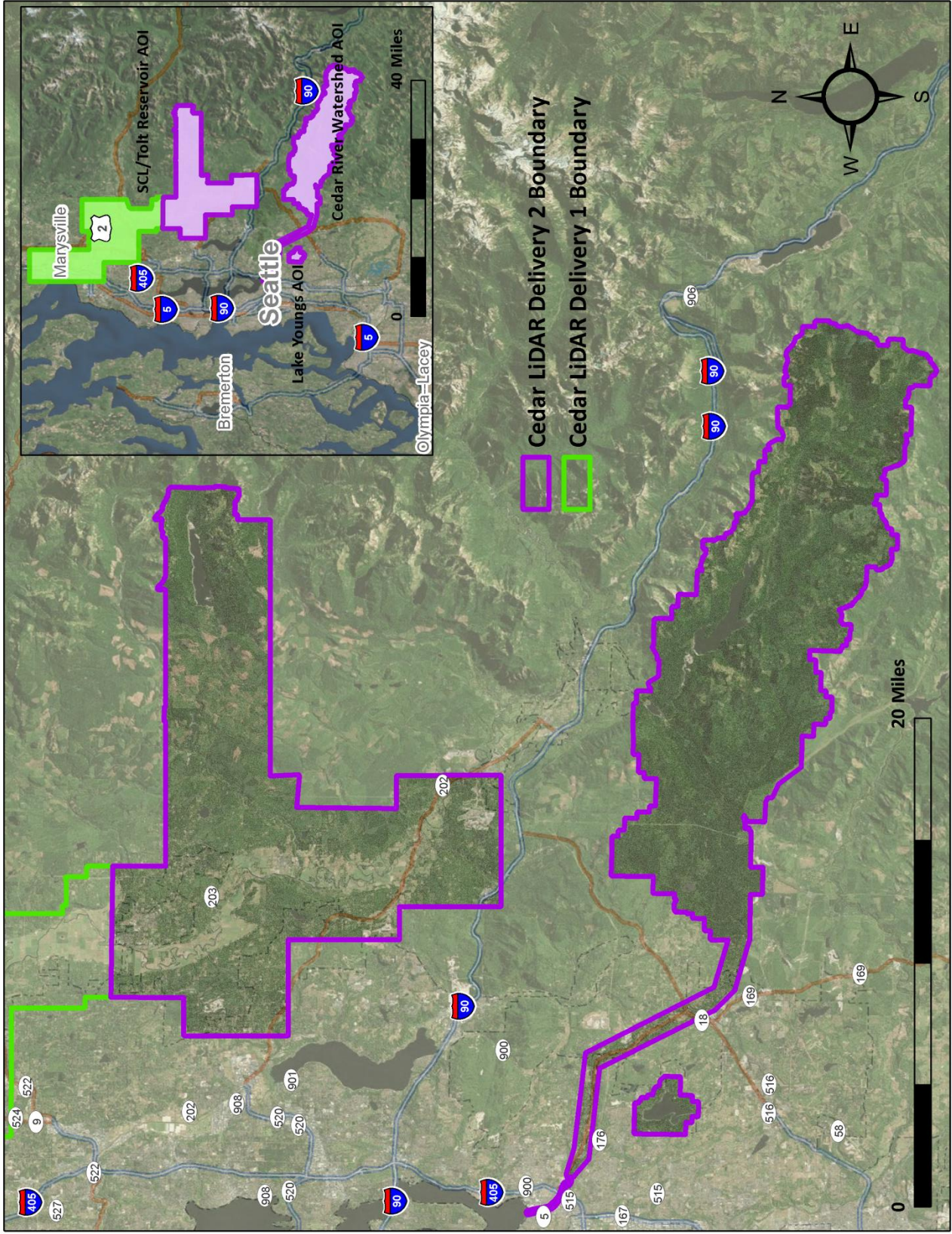


Figure 1: Location map of the Cedar Watershed LiDAR site in Washington

QSI's ground acquisition equipment set up in the Cedar Watershed LiDAR study area.



Planning

In preparation for data collection, QSI reviewed the project area and developed a specialized flight plan to ensure complete coverage of the Cedar Watershed LiDAR study area at the target point density of ≥ 8.0 points/m² (0.74 points/ft²). Acquisition parameters including orientation relative to terrain, flight altitude, pulse rate, scan angle, and ground speed were adapted in order to optimize flight paths and flight times while meeting all contract specifications.

Factors such as satellite constellation availability and weather windows must be considered during the planning stage. Any weather hazards or conditions affecting the flight were continuously monitored due to their potential impact on the daily success of airborne and ground operations. In addition, logistical considerations including field crew safety, private property access, and access restraints due to decommissioned roads were reviewed.

Ground Control

Ground control, including monumentation and ground survey points (GSP), are conducted to support the airborne acquisition process. Ground control data are used to geospatially correct the aircraft positional coordinate data and to perform quality assurance checks on final LiDAR data products.



QSI-Established Monument

Monumentation

The spatial configuration of ground survey monuments provided redundant control within 13 nautical miles of the mission areas for LiDAR flights. Monuments were also used for collection of ground survey points using real time kinematic (RTK) and post processed kinematic (PPK) survey techniques.

Monument locations were selected with consideration for satellite visibility, field crew safety, and optimal location for GSP coverage. QSI utilized two existing monuments and established fourteen new monuments for the Cedar Watershed LiDAR project (Table 3, Figure 2). New monumentation was set using 5/8" x 30" rebar topped with stamped 2" aluminum caps. QSI's professional land surveyor, Chris Brown (WA PLS# 46328 LS) oversaw and certified the establishment of all monuments.

Table 3: Monuments established for the Cedar Watershed LiDAR acquisition. Coordinates are on the NAD83 (CORS96) datum, epoch 2002.00

| Monument ID | Latitude | Longitude | Ellipsoid (meters) |
|-------------|-------------------|---------------------|--------------------|
| ASPI_CP_6 | 47° 59' 08.15207" | -122° 09' 19.19555" | -21.454 |
| CEDAR_01 | 47° 22' 19.42501" | -121° 35' 07.03373" | 1262.820 |
| CEDAR_02 | 47° 20' 17.49485" | -121° 36' 25.35834" | 1260.978 |
| CEDAR_03 | 47° 24' 15.79336" | -121° 45' 41.99196" | 972.649 |
| CEDAR_04 | 47° 23' 46.53547" | -121° 46' 37.89910" | 1142.593 |
| CEDAR_05 | 47° 25' 19.90148" | -121° 59' 08.47802" | 131.068 |
| CEDAR_06 | 47° 25' 19.30277" | -122° 04' 52.60433" | 119.181 |
| CEDAR_07 | 47° 41' 11.51397" | -121° 59' 00.88994" | -8.261 |
| CEDAR_08 | 47° 58' 33.92731" | -122° 10' 27.10333" | -21.965 |
| CEDAR_9 | 47° 48' 30.30271" | -121° 59' 57.61062" | -11.421 |
| CEDAR_10 | 47° 48' 48.46508" | -122° 03' 58.91976" | 87.133 |
| CEDAR_11 | 47° 21' 50.02557" | -121° 52' 48.83535" | 279.932 |
| CEDAR_12 | 47° 19' 50.83444" | -121° 54' 15.83024" | 237.535 |
| CEDAR_13 | 47° 41' 47.05548" | -121° 42' 05.33388" | 497.233 |
| CEDAR_14 | 47° 41' 21.03765" | -121° 42' 24.21997" | 423.276 |
| KNG_05_B | 47° 39' 31.49570" | -121° 55' 10.85389" | -4.178 |

To correct the continuously recorded onboard measurements of the aircraft position, QSI concurrently conducted multiple static Global Navigation Satellite System (GNSS) ground surveys (1 Hz recording frequency) over each monument. During post-processing, the static GPS data were triangulated with nearby Continuously Operating Reference Stations (CORS) using the Online Positioning User Service (OPUS²) for precise positioning. Multiple independent sessions over the same monument were processed to confirm antenna height measurements and to refine position accuracy.

Monuments were established according to the national standard for geodetic control networks, as specified in the Federal Geographic Data Committee (FGDC) Geospatial Positioning Accuracy Standards for geodetic networks.³ This standard provides guidelines for classification of monument quality at the 95% confidence interval as a basis for comparing the quality of one control network to another. The monument rating for this project is shown in Table 4.

Table 4: Federal Geographic Data Committee monument rating for network accuracy

| Direction | Rating |
|-------------------------------|---------|
| 1.96 * St Dev _{NE} : | 0.020 m |
| 1.96 * St Dev _z : | 0.050 m |

For the Cedar Watershed LiDAR project, the monument coordinates contributed no more than 5.3 cm of positional error to the geolocation of the final GSP and LiDAR, with 95% confidence.

Ground Survey Points (GSP)

Ground survey points were collected using real time kinematic (RTK) survey techniques. A Trimble R7 base unit was positioned at a nearby monument to broadcast a kinematic correction to a roving Trimble R8 or R10 GNSS receiver. All GSP measurements were made during periods with a Position Dilution of Precision (PDOP) of ≤ 3.0 with at least six satellites in view of the stationary and roving receivers. When collecting RTK and PPK data, the rover records data while stationary for five seconds, then calculates the pseudorange position using at least three one-second epochs. Relative errors for the position must be less than 1.5 cm horizontal and 2.0 cm vertical in order to be accepted. See Table 5 for Trimble unit specifications.

GSP were collected in areas where good satellite visibility was achieved on paved roads and other hard surfaces such as gravel or packed dirt roads. GSP measurements were not taken on highly reflective surfaces such as center line stripes or lane markings on roads due to the increased noise seen in the laser returns over these surfaces. GSP were collected within as many flightlines as possible, however the distribution of GSP depended on ground access constraints and monument locations and may not be equitably distributed throughout the study area (Figure 2).

² OPUS is a free service provided by the National Geodetic Survey to process corrected monument positions. <http://www.ngs.noaa.gov/OPUS>.

³ Federal Geographic Data Committee, Geospatial Positioning Accuracy Standards (FGDC-STD-007.2-1998). Part 2: Standards for Geodetic Networks, Table 2.1, page 2-3. <http://www.fgdc.gov/standards/projects/FGDC-standards-projects/accuracy/part2/chapter2>

Table 5: Trimble equipment identification

| Receiver Model | Antenna | OPUS Antenna ID | Use |
|-----------------|-------------------------------|-----------------|---------------|
| Trimble R7 GNSS | Zephyr GNSS Geodetic Model 2 | TRM57971.00 | Static |
| Trimble R8 | Integrated Antenna R8 Model 2 | TRM_R8_GNSS | Static, Rover |
| Trimble R10 | Integrated Antenna R10 | TRMR10 | Rover |



This photo taken by QSI ground acquisition staff shows a view of the Trimble R7 GNSS system set up on a hilltop in the Cedar Watershed project area.

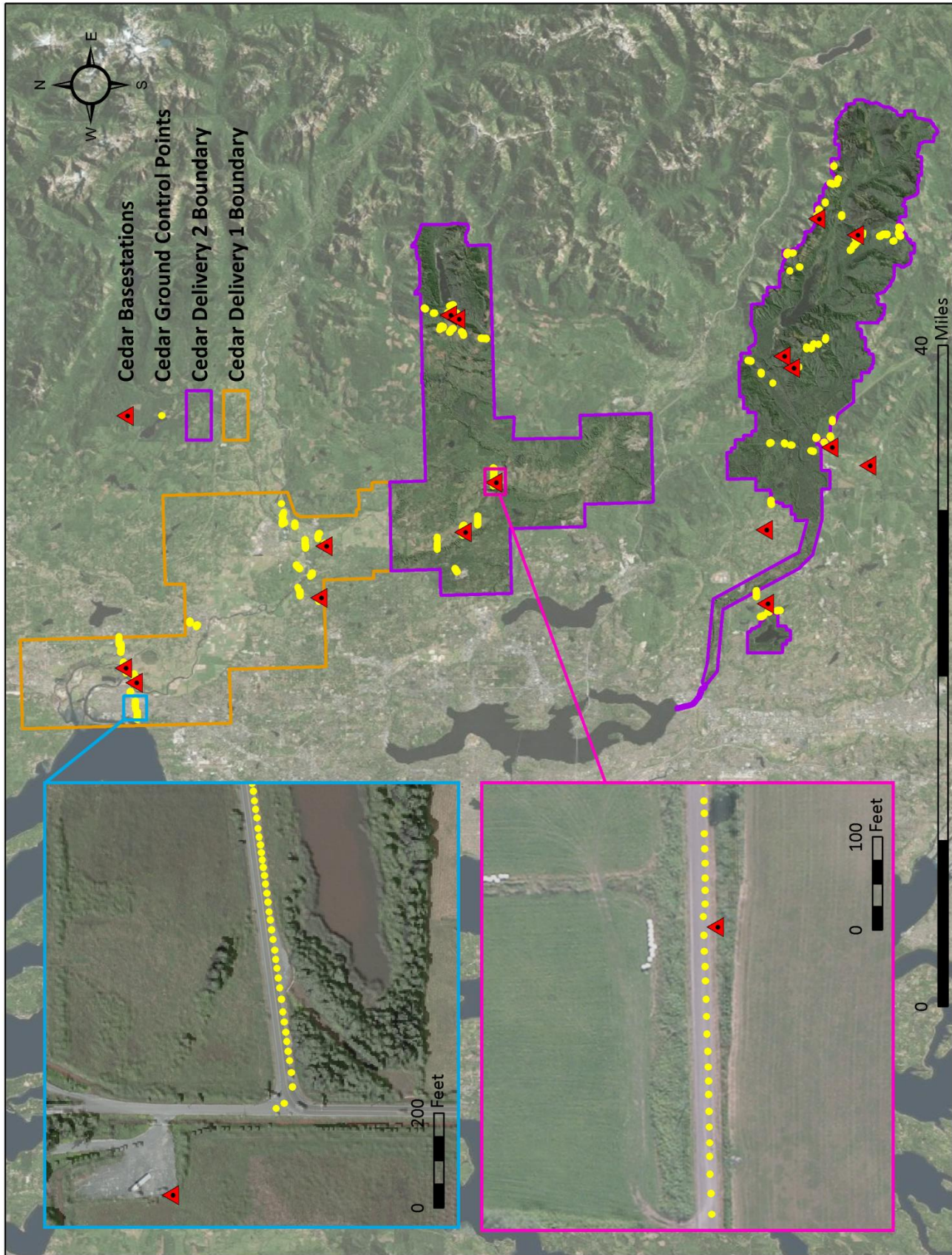


Figure 2: Ground control location map

Airborne Survey

LiDAR

The LiDAR survey was accomplished using a Leica ALS60 system mounted in a Partenavia, and a Leica ALS70 system also mounted in a Partenavia. Table 6 summarizes the settings used to yield an average pulse density of ≥ 8 pulses/m² over the Cedar Watershed LiDAR project area. It is not uncommon for some types of surfaces (e.g., dense vegetation or water) to return fewer pulses to the LiDAR sensor than the laser originally emitted. The Leica ALS60 laser system records up to four range measurements (returns) per pulse, and the Leica ALS70 laser system can record unlimited range measurements (returns) per pulse, but typically does not record more than 7 returns per pulse. All discernible laser returns were processed for the output dataset. The discrepancy between native and delivered density will vary depending on terrain, land cover, and the prevalence of water bodies.

Table 6: LiDAR specifications and survey settings for the Cedar River Watershed Delivery 2

| LiDAR Survey Settings & Specifications | | | | |
|--|--|---|---|---------------------------------|
| Acquisition Dates | October 29 – 30, 2013 November 1, 3 – 4, 2013 | December 3 - 5, 2013 | December 4, 2013 | December 11 - 12, 2013 |
| Aircraft Used | Partenavia | Partenavia | Partenavia | Partenavia |
| Sensor | Leica ALS60 | Leica ALS70 | Leica ALS70 | Leica ALS60 |
| Survey Altitude (AGL) | 1,100 m | 1,300 m | 1,600 m | 900 m |
| Target Pulse Rate | 85 - 93.3 kHz | 201 – 209.4 kHz | 165 - 175 kHz | 95 – 106 kHz |
| Sensor Configuration | Single Pulse in Air (SPiA) | Single Pulse in Air (SPiA) | Single Pulse in Air (SPiA) | Single Pulse in Air (SPiA) |
| Laser Pulse Diameter | 26 cm | 30 cm | 37 cm | 21 cm |
| Mirror Scan Rate | 53.9 Hz | 42.7 Hz | 36.2 Hz | 65.9 Hz |
| Field of View | 28° | 30° | 30° | 26° |
| GPS Baselines | ≤13 nm | ≤13 nm | ≤13 nm | ≤13 nm |
| GPS PDOP | ≤3.0 | ≤3.0 | ≤3.0 | ≤3.0 |
| GPS Satellite Constellation | ≥6 | ≥6 | ≥6 | ≥6 |
| Maximum Returns | 4 | Unlimited, but typically no more than 5 | Unlimited, but typically no more than 5 | 4 |
| Intensity | 8-bit | 8-bit | 8-bit | 8-bit |
| Resolution/Density | Average 8 pulses/m ² | Average 8 pulses/m ² | Average 8 pulses/m ² | Average 8 pulses/m ² |
| Accuracy | RMSE _z ≤ 15 cm | RMSE _z ≤ 15 cm | RMSE _z ≤ 15 cm | RMSE _z ≤ 15 cm |

| LiDAR Survey Settings & Specifications | | | |
|--|---------------------------------|---|---|
| Acquisition Dates | December 16, 2013 | February 3 - 7, 2014 | June 22, 23, 30, 2014 July 2, 5, 6, 7, 8, 2014 |
| Aircraft Used | Partenavia | Partenavia | Piper Navajo |
| Sensor | Leica ALS60 | Leica ALS70 | Leica ALS70 |
| Survey Altitude (AGL) | 1,400 m | 1,000 – 1,300 m | Varied |
| Target Pulse Rate | 152 kHz | 201 – 275.6 kHz | 215.2 kHz |
| Sensor Configuration | Multiple Pulse in Air (MPiA) | Single Pulse in Air (SPiA) | Single Pulse in Air (SPiA) |
| Laser Pulse Diameter | 32 cm | 23 – 30 cm | 30 cm |
| Mirror Scan Rate | 66.2 Hz | 42.7 – 59.7 Hz | 53 Hz |
| Field of View | 24° | 30° | 28° |
| GPS Baselines | ≤13 nm | ≤13 nm | ≤13 nm |
| GPS PDOP | ≤3.0 | ≤3.0 | ≤3.0 |
| GPS Satellite Constellation | ≥6 | ≥6 | ≥6 |
| Maximum Returns | 4 | Unlimited, although typically not more than 5 | Unlimited, although typically not more than 5 |
| Intensity | 8-bit | 8-bit | 8-bit |
| Resolution/Density | Average 8 pulses/m ² | Average 8 pulses/m ² | Average 8 pulses/m ² |
| Accuracy | RMSE _z ≤ 15 cm | RMSE _z ≤ 15 cm | RMSE _z ≤ 15 cm |

All areas were surveyed with an opposing flight line side-lap of ≥50% (≥100% overlap) in order to reduce laser shadowing and increase surface laser painting. To accurately solve for laser point position (geographic coordinates x, y and z), the positional coordinates of the airborne sensor and the attitude of the aircraft were recorded continuously throughout the LiDAR data collection mission. Position of the aircraft was measured twice per second (2 Hz) by an onboard differential GPS unit, and aircraft attitude was measured 200 times per second (200 Hz) as pitch, roll and yaw (heading) from an onboard inertial measurement unit (IMU). To allow for post-processing correction and calibration, aircraft and sensor position and attitude data are indexed by GPS time. Flightline paths and dates are shown in Figure 3.

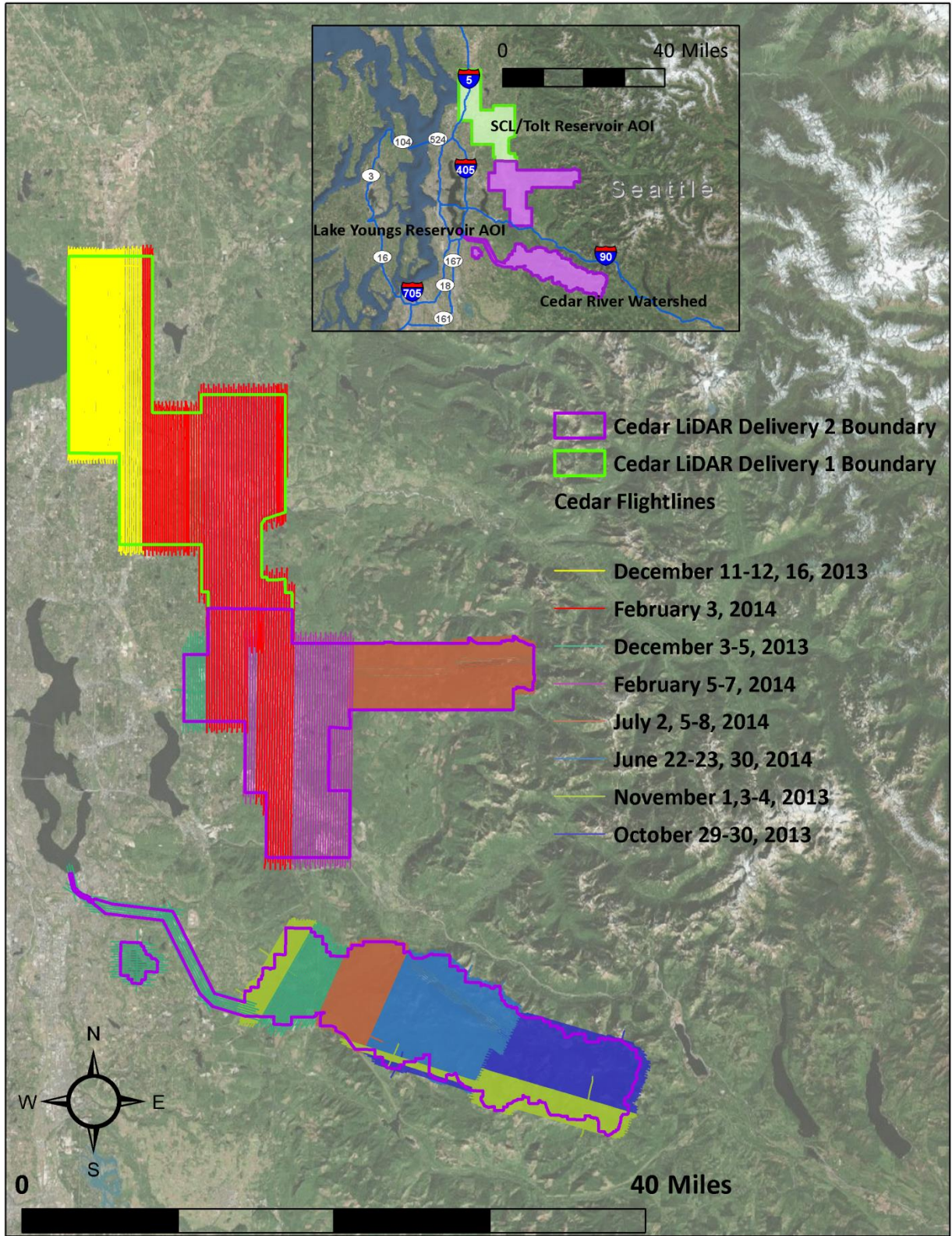
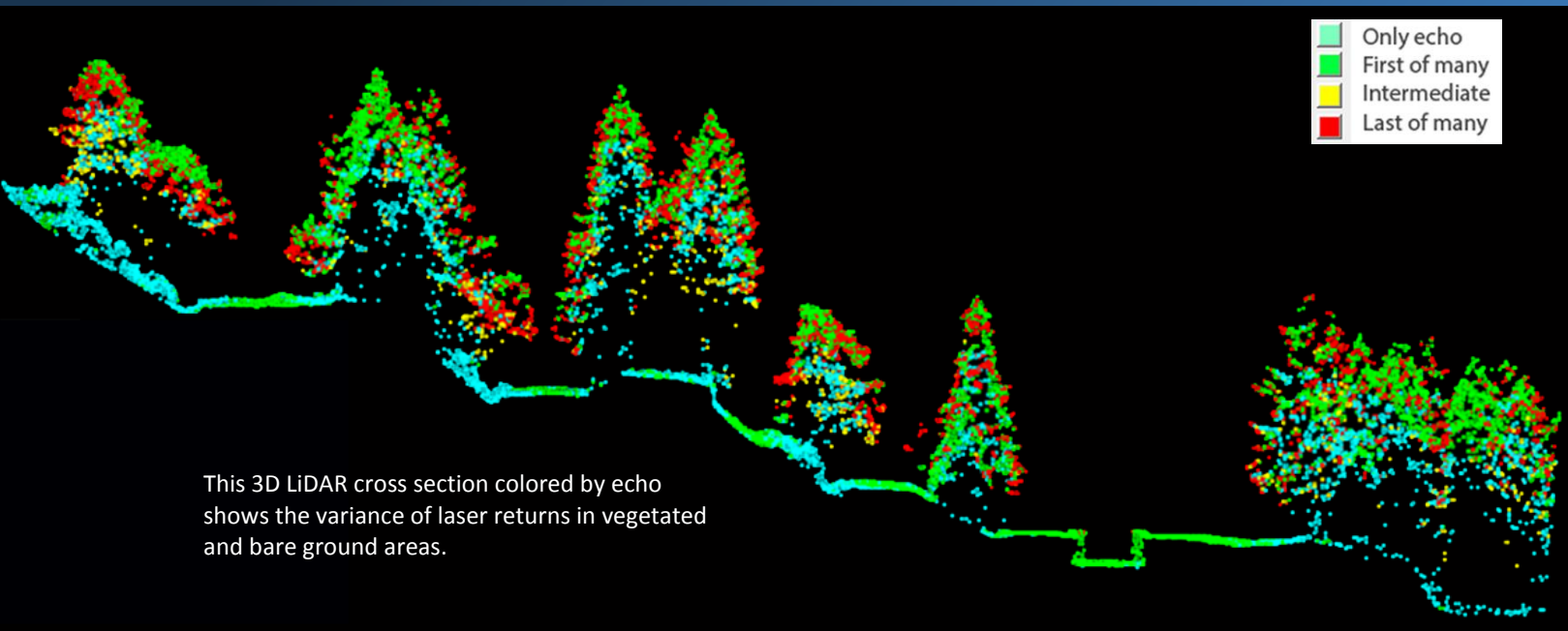


Figure 3: Cedar Watershed LiDAR flight lines by date of acquisition



LiDAR Data

Upon completion of data acquisition, QSI processing staff initiated a suite of automated and manual techniques to process the data into the requested deliverables. Processing tasks included GPS control computations, smoothed best estimate trajectory (SBET) calculations, kinematic corrections, calculation of laser point position, sensor and data calibration for optimal relative and absolute accuracy, and LiDAR point classification (Table 7). Processing methodologies were tailored for the landscape. Brief descriptions of these tasks are shown in Table 8.

Table 7: ASPRS LAS classification standards applied to the Cedar Watershed LiDAR dataset

| Classification Number | Classification Name | Classification Description |
|-----------------------|-----------------------|---|
| 1 | Default/ Unclassified | Laser returns that are not included in the ground class, composed of vegetation and man-made structures |
| 2 | Ground | Bare earth ground, determined by a number of automated and manual cleaning algorithms |

Table 8: LiDAR processing workflow

| LiDAR Processing Step | Software Used |
|---|--|
| Resolve kinematic corrections for aircraft position data using kinematic aircraft GPS and static ground GPS data. | Waypoint GPS v.8.3 Trimble Business Center v.3.10 Geographic Calculator 2013 |
| Develop a smoothed best estimate of trajectory (SBET) file that blends post-processed aircraft position with sensor head position and attitude recorded throughout the survey. | IPAS TC v.3.1 |
| Calculate laser point position by associating SBET position to each laser point return time, scan angle, intensity, etc. Create raw laser point cloud data for the entire survey in *.las (ASPRS v. 1.2) format. Convert data to orthometric elevations by applying a geoid03 correction. | ALS Post Processing Software v.2.74 |
| Import raw laser points into manageable blocks (less than 500 MB) to perform manual relative accuracy calibration and filter erroneous points. Classify ground points for individual flight lines | TerraScan v.14.001 |
| Using ground classified points per each flight line, test the relative accuracy. Perform automated line-to-line calibrations for system attitude parameters (pitch, roll, heading), mirror flex (scale) and GPS/IMU drift. Calculate calibrations on ground classified points from paired flight lines and apply results to all points in a flight line. Use every flight line for relative accuracy calibration. | TerraMatch v.14.001 |
| Remove individual line classifications and reclassify entire calibrated dataset to ground and other client designated ASPRS classifications (Table 7). Assess statistical absolute accuracy via direct comparisons of final ground classified points to ground control survey data. | TerraScan v.14.001 TerraModeler v. 14.001 |
| Generate bare earth models as triangulated surfaces. Generate highest hit models as a surface expression of all classified points Export all surface models as ESRI GRIDs at a 3 foot pixel resolution. | TerraScan v. 14.001 ArcMap v. 10.1 TerraModeler v. 14.001 |
| Export intensity images as GeoTIFFs at a 1.5 foot pixel resolution. | TerraScan v. 14.001 ArcMap v. 10.1 TerraModeler v. 14.001 |

View looking North/northeast over the Cedar River located South/southeast of Hobart, Washington. This image was created from the gridded LiDAR surface colored by elevation.



LiDAR Density

The acquisition parameters were designed to acquire an average first-return density of 8 points/m² (0.74 points/ft²). First return density describes the density of pulses emitted from the laser that return at least one echo to the system. Multiple returns from a single pulse are not considered in first return density analysis. Pulse density distribution will vary within the study area due to laser scan pattern and flight conditions. Additionally, some types of surfaces (e.g., breaks in terrain, water and steep slopes) may return fewer pulses than originally emitted by the laser. First returns typically reflect off the highest feature on the landscape within the footprint of the pulse. In forested or urban areas the highest feature could be a tree, building or power line, while in areas of unobstructed ground, the first return represents the bare earth surface.

The density of ground-classified LiDAR returns was also analyzed for this project. Ground-classified return density is dictated by a combination of variables. Terrain character, land cover, and ground surface reflectivity all influence the density of ground surface returns. In vegetated areas fewer pulses may penetrate the canopy, resulting in lower ground density.

The average first-return density of LiDAR data for the Cedar Watershed LiDAR project was 1.15 points/ft² (12.41 points/m²) while the average ground classified density was 0.25 points/ft² (2.67 points/m²) (Table 9). The statistical distribution of first return densities (Figure 4) and classified ground return densities (Figure 5) are portrayed. Also presented are the spatial distribution of average first return densities (Figure 6) and ground return densities (Figure 7) for each 30 m by 30 m cell. See Appendix B for additional density distributions by AOI.

Table 9: Average LiDAR point densities

| Classification | Cedar River Watershed & Floodplain | Lake Youngs Reservoir | SCL/Tolt Reservoir | Cumulative Point Density |
|--------------------------|--|--|--|--|
| First-Return | 1.37 points/ft ² 14.70 points/m ² | 1.08 points/ft ² 11.65 points/m ² | 1.24 points/ft ² 13.38 points/m ² | 1.28 points/ft ² 13.78 points/m ² |
| Ground Classified | 0.09 points/ft ² 1.00 points/m ² | 0.13 points/ft ² 1.35 points/m ² | 0.20 points/ft ² 2.18 points/m ² | 0.17 points/ft ² 1.80 points/m ² |

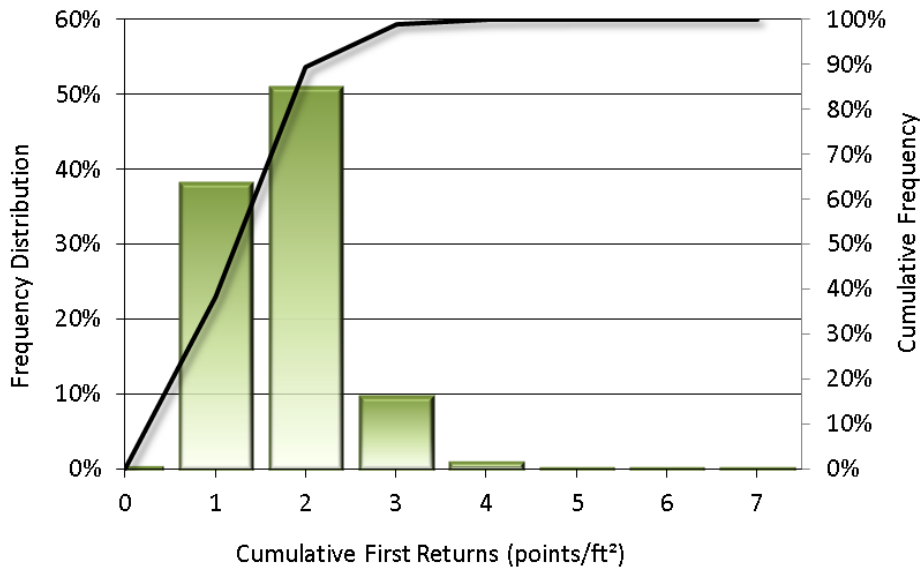


Figure 4: Frequency distribution of first return densities of the 30 x 30 m gridded study area

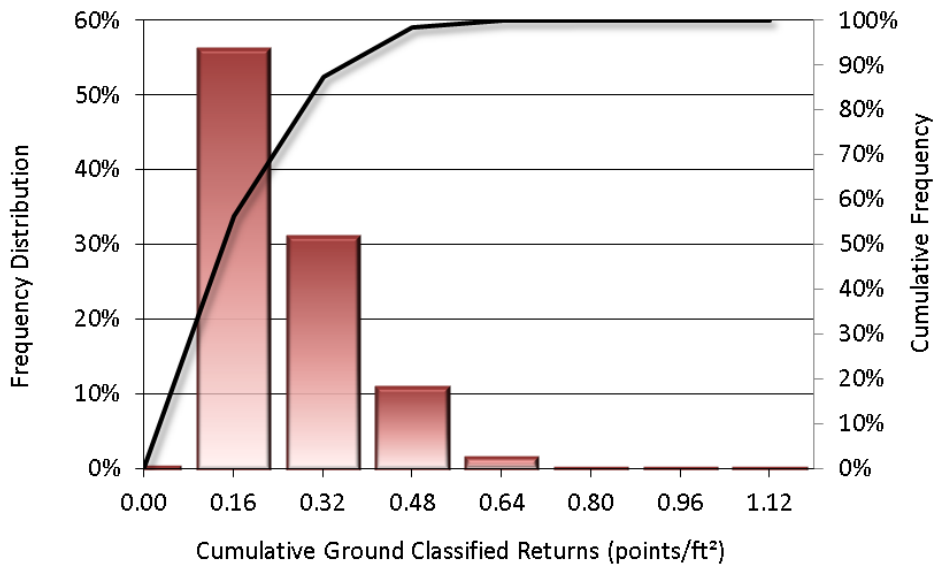


Figure 5: Frequency distribution of ground return densities of the 30 x 30 m gridded study area

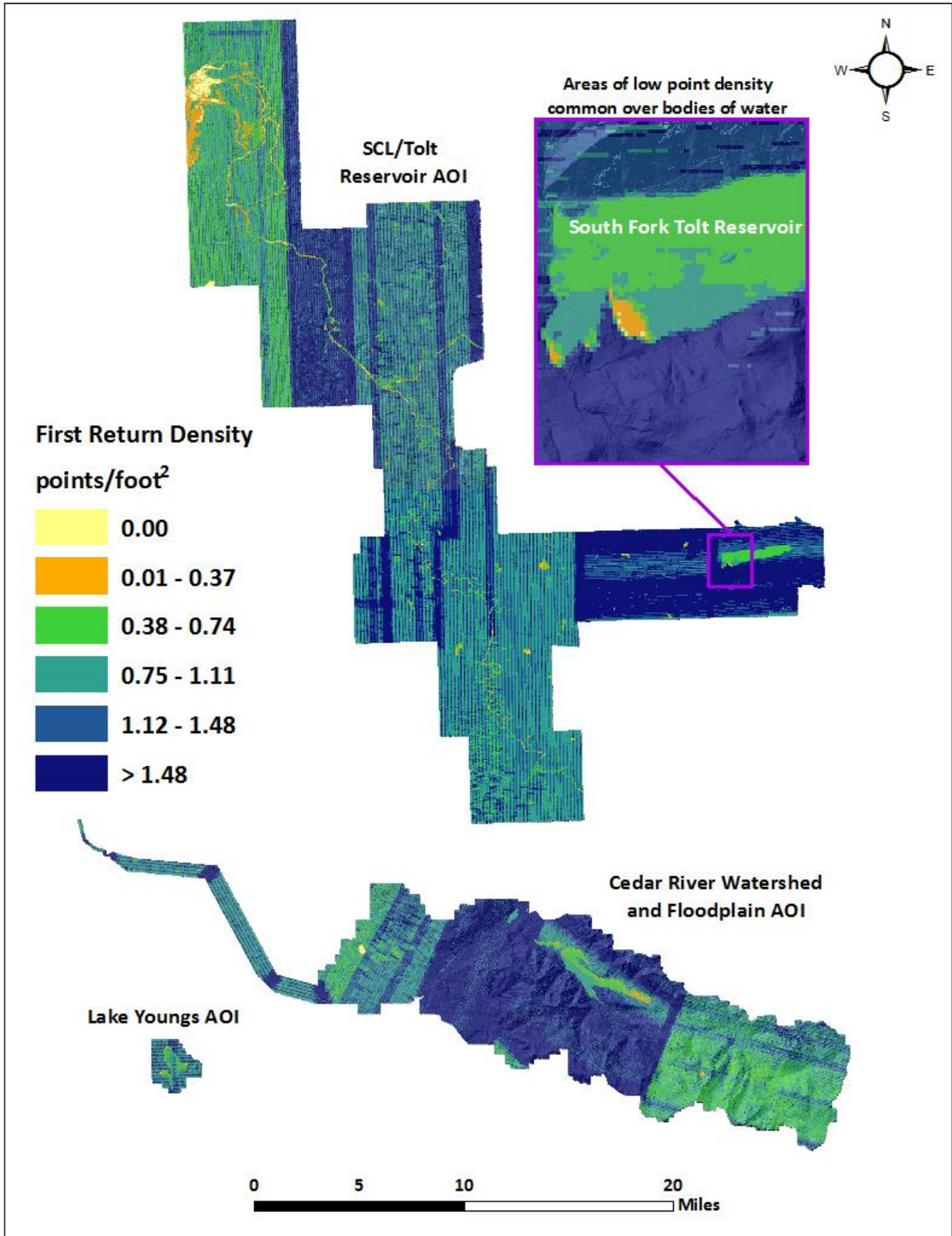


Figure 6: First return density map for the Cedar Watershed LiDAR site (30 m by 30 m cells)

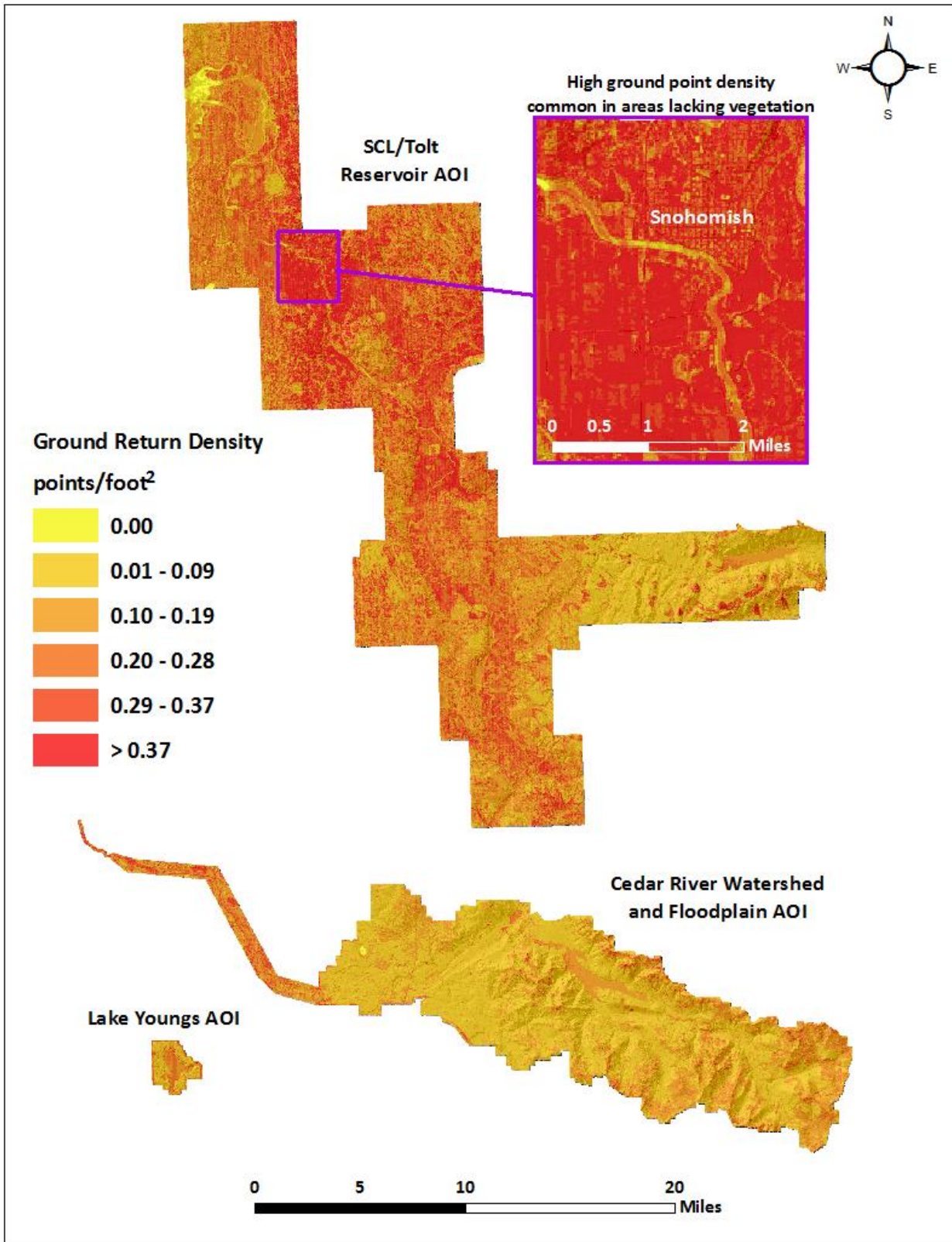


Figure 7: Ground density map for the Cedar Watershed LiDAR site (30 m by 30 m cells)

LiDAR Accuracy Assessments

The accuracy of the LiDAR data collection can be described in terms of absolute accuracy (the consistency of the data with external data sources) and relative accuracy (the consistency of the dataset with itself). See Appendix A for further information on sources of error and operational measures used to improve relative accuracy.

LiDAR Absolute Accuracy

Absolute accuracy was assessed using Fundamental Vertical Accuracy (FVA) reporting designed to meet guidelines presented in the FGDC National Standard for Spatial Data Accuracy⁴. FVA compares known RTK ground control point data collected on open, bare earth surfaces with level slope (<20°) to the final triangulated ground surface generated by the LiDAR points. FVA is a measure of the accuracy of LiDAR point data in open areas where the LiDAR system has a “very high probability” of measuring the ground surface and is evaluated at the 95% confidence interval (1.96 * RMSE), as shown in Table 10. For the Cedar River Watershed project, FVA was assessed using RTK ground control point data that was used in the calibration and post-processing of the LiDAR point cloud.

The mean and standard deviation (sigma σ) of divergence of the ground surface model from ground survey point coordinates are also considered during accuracy assessment. These statistics assume the error for x, y and z is normally distributed, and therefore the skew and kurtosis of distributions are also considered when evaluating error statistics. For the Cedar Watershed LiDAR survey, 4,093 ground survey points were collected in total resulting in a fundamental vertical accuracy of 0.182 feet (0.055 meters) (Figure 8). See Appendix B for additional absolute accuracy frequency histograms by AOI.

Table 10: Absolute accuracy

| Absolute Accuracy | | | | |
|--|------------------------------------|-----------------------|-----------------------|-----------------------|
| | Cedar River Watershed & Floodplain | Lake Youngs Reservoir | SCL/Tolt Reservoir | Cumulative Accuracy |
| Sample | 1,555 points | 132 points | 2,406 points | 4,093 points |
| FVA (1.96*RMSE) | 0.210 ft 0.064 m | 0.126 ft 0.038 m | 0.164 ft 0.050 m | 0.182 ft 0.055 m |
| Average | -0.022 ft -0.007 m | 0.006 ft 0.002 m | -0.024 ft -0.007 m | -0.023 ft -0.007 m |
| Median | -0.016 ft -0.005 m | 0.007 ft 0.002 m | -0.023 ft -0.007 m | -0.020 ft -0.006 m |
| RMSE | 0.107 ft 0.033 m | 0.064 ft 0.020 m | 0.084 ft 0.026 m | 0.093 ft 0.028 m |
| Standard Deviation (1σ) | 0.105 ft 0.032 m | 0.064 ft 0.020 m | 0.080 ft 0.024 m | 0.090 ft 0.027 m |

⁴ Federal Geographic Data Committee, Geospatial Positioning Accuracy Standards (FGDC-STD-007.3-1998). Part 3: National Standard for Spatial Data Accuracy. <http://www.fgdc.gov/standards/projects/FGDC-standards-projects/accuracy/part3/chapter3>

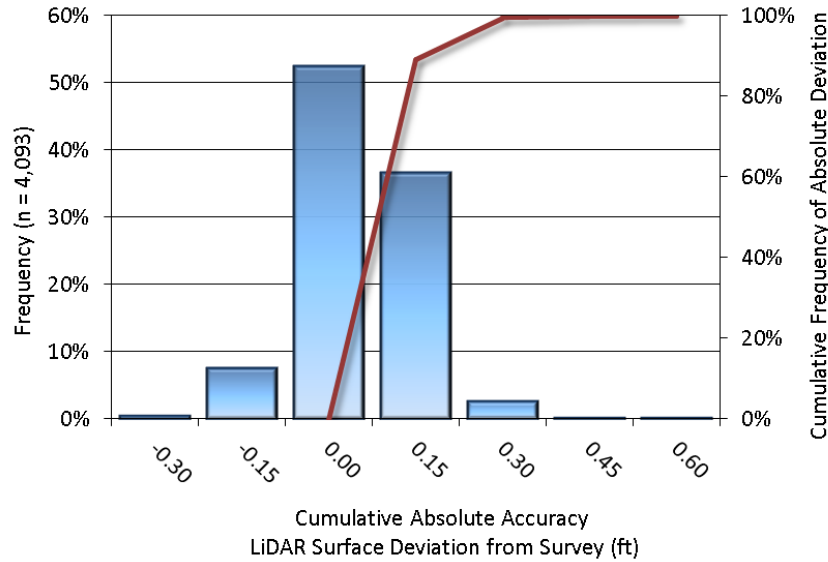


Figure 8: Frequency histogram for LiDAR surface deviation from ground survey point values

LiDAR Vertical Relative Accuracy

Relative vertical accuracy refers to the internal consistency of the data set as a whole: the ability to place an object in the same location given multiple flight lines, GPS conditions, and aircraft attitudes. When the LiDAR system is well calibrated, the swath-to-swath vertical divergence is low (<0.10 meters). The relative vertical accuracy is computed by comparing the ground surface model of each individual flight line with its neighbors in overlapping regions. The average (mean) line to line relative vertical accuracy for the Cedar Watershed LiDAR project was 0.126 feet (0.039 meters) (Table 11, Figure 9). The vertical difference between lines is expressed as absolute deviation without positive or negative direction. Therefore the standard deviation below describes the distribution about the mean, while the RMSE describes the vertical deviation as error compared to zero, which would represent no vertical discrepancy between flightlines.

Table 11: Relative accuracy

| Relative Accuracy | | | | |
|-------------------|------------------------------------|-----------------------|--------------------|------------------------------|
| | Cedar River Watershed & Floodplain | Lake Youngs Reservoir | SCL/Tolt Reservoir | Cumulative Relative Accuracy |
| Sample | 370 surfaces | 19 surfaces | 338 surfaces | 727 surfaces |
| Average | 0.086 ft | 0.142 ft | 0.127 ft | 0.126 ft |
| | 0.026 m | 0.043 m | 0.039 m | 0.039 m |
| Median | 0.099 ft | 0.141 ft | 0.134 ft | 0.115 ft |
| | 0.030 m | 0.043 m | 0.041 m | 0.035 m |
| RMSE | 0.100 ft | 0.141 ft | 0.147 ft | 0.125 ft |
| | 0.031 m | 0.043 m | 0.045 m | 0.038 m |

| | | | | |
|--------------------------------|---------------------|---------------------|---------------------|---------------------|
| Standard Deviation (1σ) | 0.023 ft 0.007 m | 0.011 ft 0.003 m | 0.034 ft 0.010 m | 0.036 ft 0.011 m |
| 1.96σ | 0.044 ft 0.013 m | 0.021 ft 0.006 m | 0.066 ft 0.020 m | 0.070 ft 0.021 m |

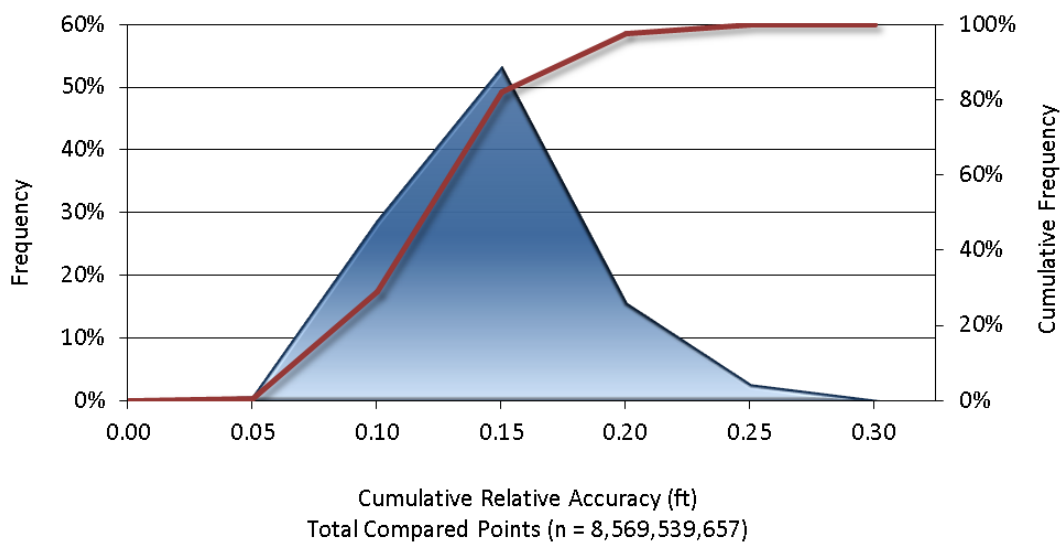


Figure 9: Frequency plot for relative vertical accuracy between flight lines

CERTIFICATIONS

Quantum Spatial provided LiDAR services for the Cedar Watershed project as described in this report.

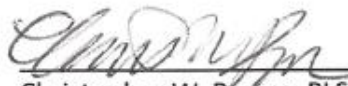
I, Kris Fausti, have reviewed the attached report for completeness and hereby state that it is a complete and accurate report of this project.



Kris Fausti
Operations Manager
Quantum Spatial

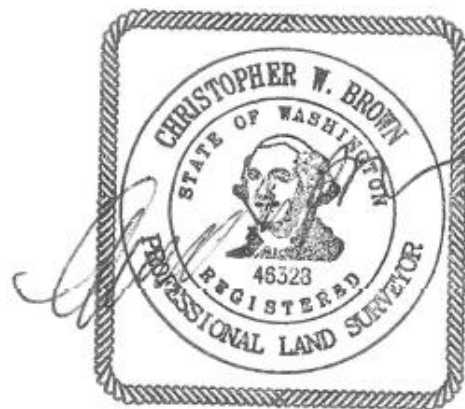
I, Christopher W. Brown, being duly registered as a Professional Land Surveyor in and by the state of Washington, say that I hereby certify the methodologies, LiDAR project, Static GNSS occupations on the Base Stations used during airborne flights and RTK survey on hard-surface, were performed using commonly accepted Standard Practices. Field work for this report was conducted between October 29, 2013 and July 8, 2014.

Accuracy statistics shown in the Accuracy Section of this Report have been reviewed by me and found to meet the "National Standard for Spatial Data Accuracy".



9/4/2014

Christopher W. Brown, PLS Oregon & Washington
Quantum Spatial
Portland, OR 97204



Renews: 12/21/2014

SELECTED IMAGES

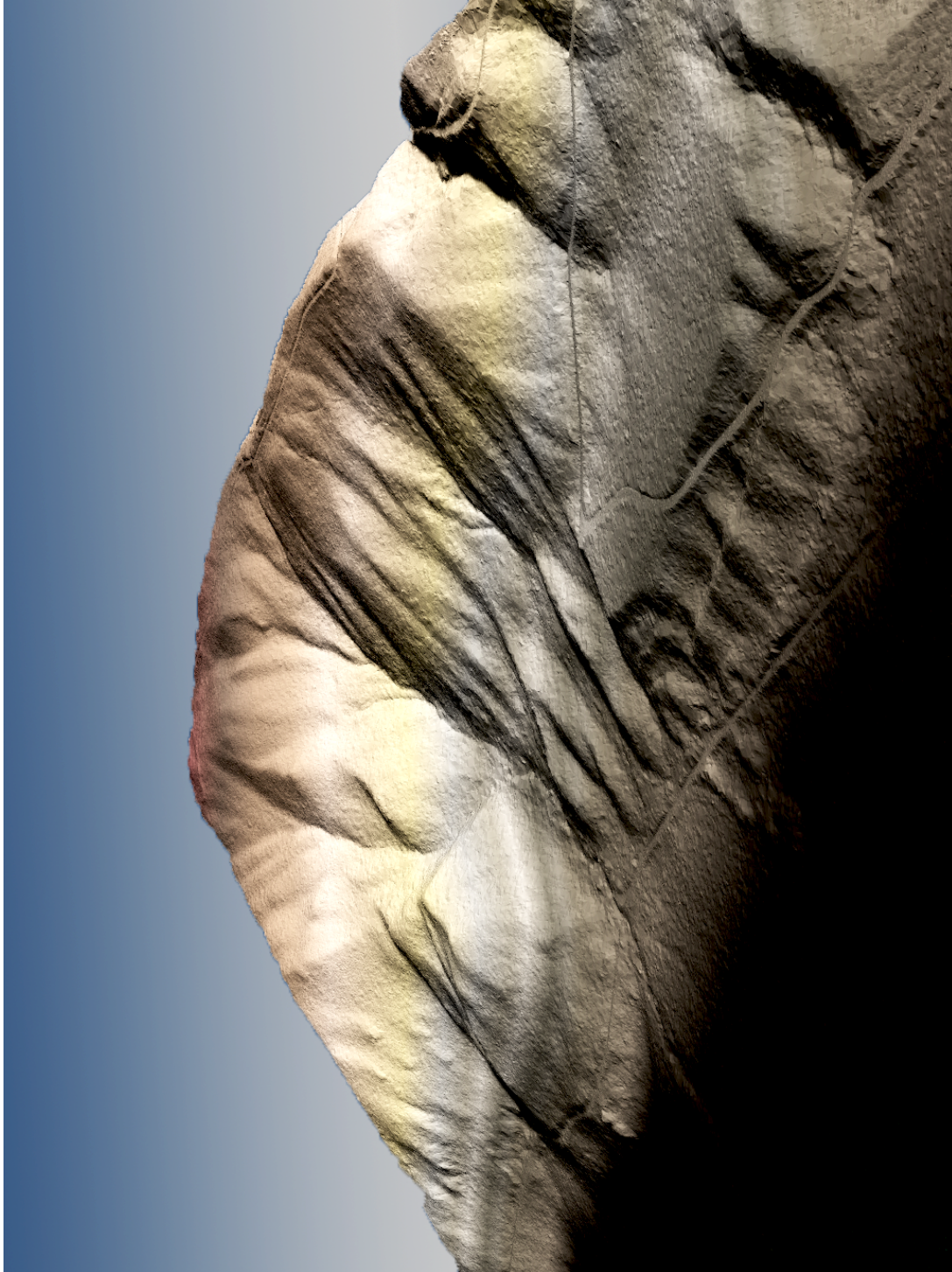


Figure 10: A view looking northwest toward Lookout Mountain. The image was created from the gridded LiDAR surface colored by elevation.

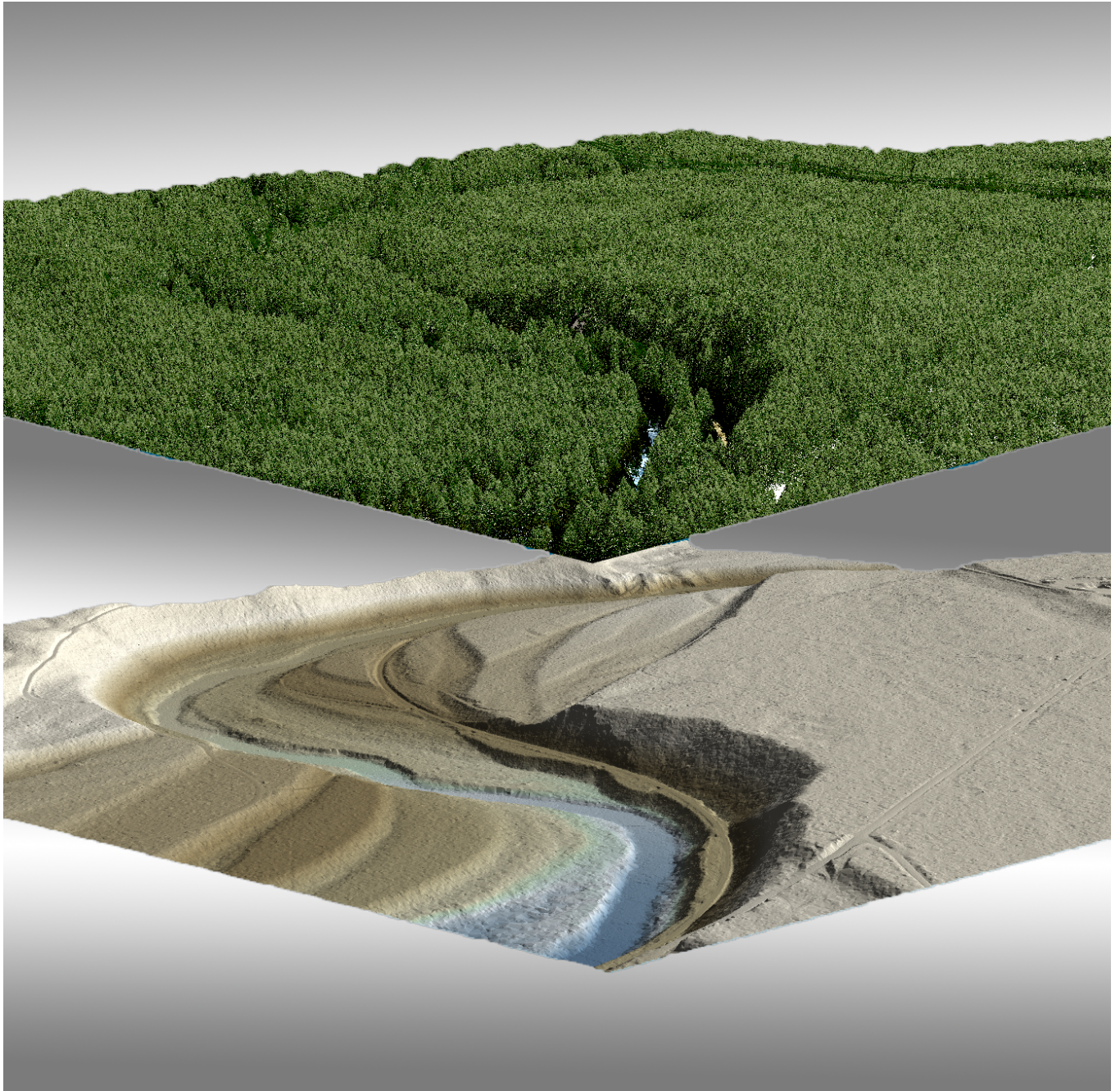


Figure 11: A view looking Northeast at a meander in the Cedar River, approximately 6 miles southwest of Rattlesnake Lake. These images were created from the gridded LiDAR surface colored by elevation overlaid with the LiDAR point cloud in the top image.

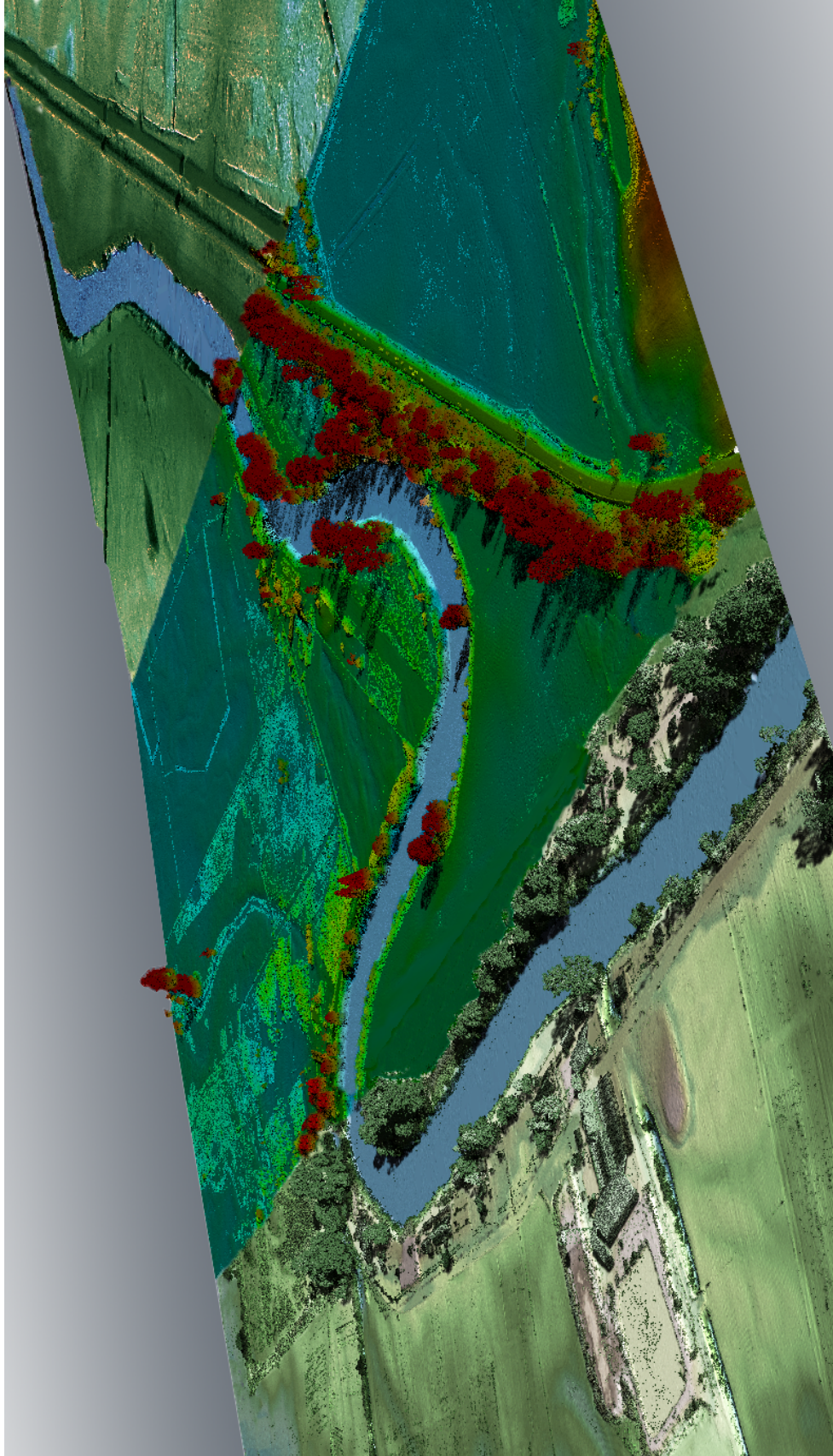


Figure 12: A view looking northeast over the Cedar River located North of Duvall, Washington. The images were created with the gridded LiDAR surface, with the left image draped with the 3-D LiDAR point cloud and the LiDAR point cloud in the center image colored by intensity and elevation.

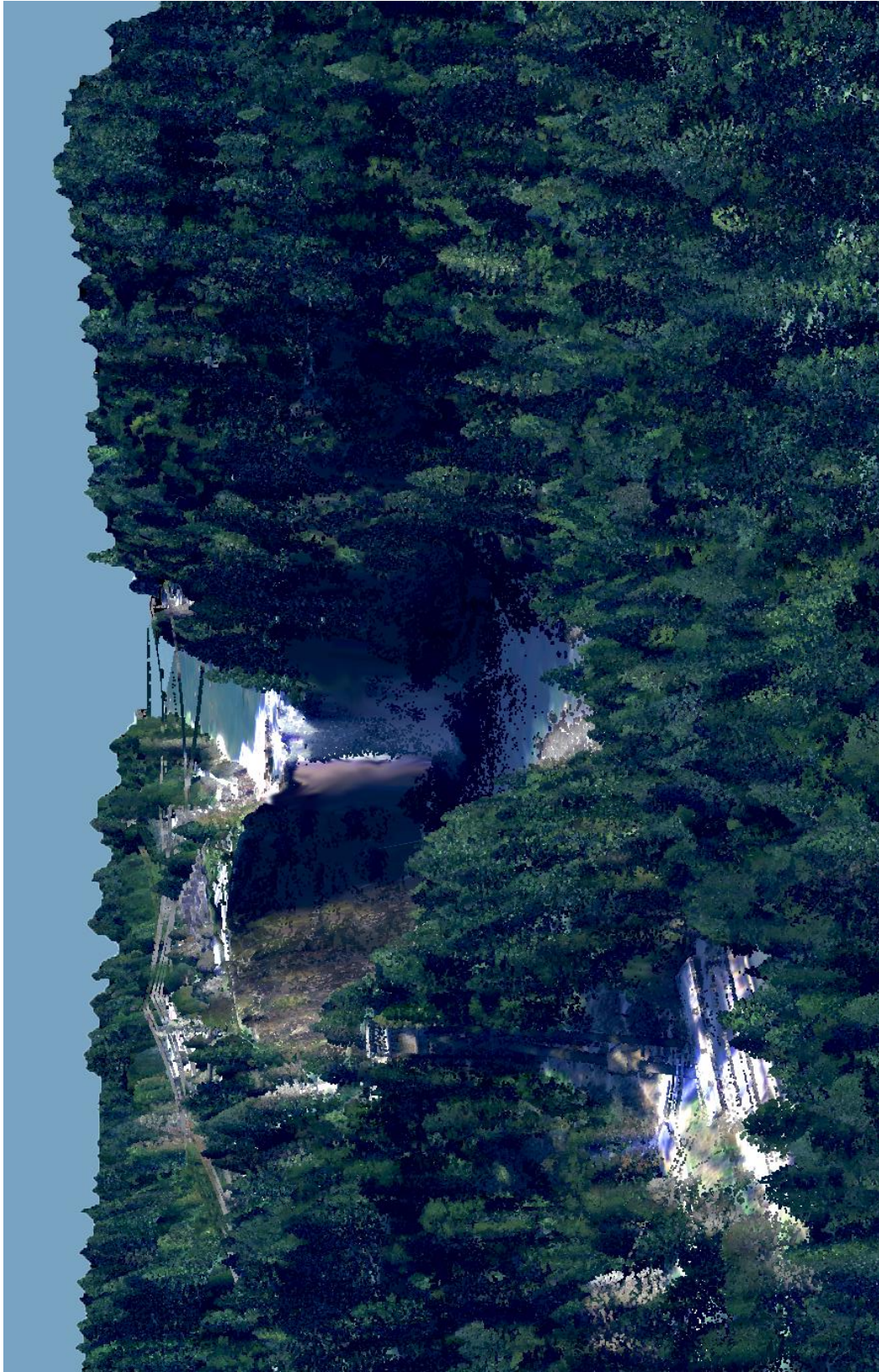


Figure 13: View looking southeast at Snoqualmie Falls. The image was created from National Agriculture Imagery Program (NAIP) imagery draped over the gridded LiDAR surface and overlaid with the LiDAR point cloud.

1-sigma (σ) Absolute Deviation: Value for which the data are within one standard deviation (approximately 68th percentile) of a normally distributed data set.

1.96-sigma (σ) Absolute Deviation: Value for which the data are within two standard deviations (approximately 95th percentile) of a normally distributed data set.

Accuracy: The statistical comparison between known (surveyed) points and laser points. Typically measured as the standard deviation (σ) and root mean square error (RMSE).

Absolute Accuracy: The vertical accuracy of LiDAR data is described as the mean and standard deviation (σ) of divergence of LiDAR point coordinates from RTK ground survey point coordinates. To provide a sense of the model predictive power of the dataset, the root mean square error (RMSE) for vertical accuracy is also provided. These statistics assume the error distributions for x, y and z are normally distributed, and thus we also consider the skew and kurtosis of distributions when evaluating error statistics.

Relative Accuracy: Relative accuracy refers to the internal consistency of the data set; i.e., the ability to place a laser point in the same location over multiple flight lines, GPS conditions and aircraft attitudes. Affected by system attitude offsets, scale and GPS/IMU drift, internal consistency is measured as the divergence between points from different flight lines within an overlapping area. Divergence is most apparent when flight lines are opposing. When the LiDAR system is well calibrated, the line-to-line divergence is low (<10 cm).

Root Mean Square Error (RMSE): A statistic used to approximate the difference between real-world points and the LiDAR points. It is calculated by squaring all the values, then taking the average of the squares and taking the square root of the average.

Data Density: A common measure of LiDAR resolution, measured as points per square meter.

DTM / DEM: These often-interchanged terms refer to models made from laser points. The digital elevation model (DEM) refers to all surfaces, including bare ground and vegetation, while the digital terrain model (DTM) refers only to those points classified as ground.

Intensity Values: The peak power ratio of the laser return to the emitted laser, calculated as a function of surface reflectivity.

Laser Noise: For any given target, laser noise is the breadth of the data cloud per laser return (i.e., first to last). Lower intensity surfaces (e.g., roads, rooftops, still/calm water) experience higher laser noise.

Nadir: A single point or locus of points on the surface of the earth directly below a sensor as it progresses along its flight line.

Overlap: The area shared between flight lines, typically measured in percent. 100% overlap is essential to ensure complete coverage and reduce laser shadows.

Pulse Rate (PR): The rate at which laser pulses are emitted from the sensor; typically measured in thousands of pulses per second (kHz).

Pulse Returns: For every laser pulse emitted, the number of wave forms reflected back to the sensor. Portions of the wave form that return first are the highest element in multi-tiered surfaces such as vegetation. Portions of the wave form that return last are the lowest element in multi-tiered surfaces.

Real-Time Kinematic (RTK) Survey: A type of surveying conducted with a GPS base station deployed over a known monument with a radio connection to a GPS rover. Both the base station and rover receive differential GPS data and the baseline correction is solved between the two. This type of ground survey is accurate to 1.5 cm or less.

Scan Angle: The angle from nadir to the edge of the scan, measured in degrees. Laser point accuracy typically decreases as scan angles increase.

Spot Spacing: Also a measure of LiDAR resolution, measured as the average distance between laser points.

Native Density: The number of pulses emitted by the LiDAR system, commonly expressed in pulses per square meter (ppsm).

APPENDIX A - ACCURACY CONTROLS

Relative Accuracy Calibration Methodology:

Manual System Calibration: Calibration procedures for each mission require solving geometric relationships that relate measured swath-to-swath deviations to misalignments of system attitude parameters. Corrected scale, pitch, roll and heading offsets were calculated and applied to resolve misalignments. The raw divergence between lines was computed after the manual calibration was completed and reported for each survey area.

Automated Attitude Calibration: All data were tested and calibrated using TerraMatch automated sampling routines. Ground points were classified for each individual flight line and used for line-to-line testing. System misalignment offsets (pitch, roll and heading) and scale were solved for each individual mission and applied to respective mission datasets. The data from each mission were then blended when imported together to form the entire area of interest.

Automated Z Calibration: Ground points per line were used to calculate the vertical divergence between lines caused by vertical GPS drift. Automated Z calibration was the final step employed for relative accuracy calibration.

LiDAR accuracy error sources and solutions:

| Type of Error | Source | Post Processing Solution |
|---------------------------|------------------------------|---|
| GPS (Static/Kinematic) | Long Base Lines | None |
| | Poor Satellite Constellation | None |
| | Poor Antenna Visibility | Reduce Visibility Mask |
| Relative Accuracy | Poor System Calibration | Recalibrate IMU and sensor offsets/settings |
| | Inaccurate System | None |
| Laser Noise | Poor Laser Timing | None |
| | Poor Laser Reception | None |
| | Poor Laser Power | None |
| | Irregular Laser Shape | None |

Operational measures taken to improve relative accuracy:

Low Flight Altitude: Terrain following was employed to maintain a constant above ground level (AGL). Laser horizontal errors are a function of flight altitude above ground (about 1/3000th AGL flight altitude).

Focus Laser Power at narrow beam footprint: A laser return must be received by the system above a power threshold to accurately record a measurement. The strength of the laser return is a function of laser emission power, laser footprint, flight altitude and the reflectivity of the target. While surface reflectivity cannot be controlled, laser power can be increased and low flight altitudes can be maintained.

Reduced Scan Angle: Edge-of-scan data can become inaccurate. The scan angle was reduced to a maximum of $\pm 15^\circ$ from nadir, creating a narrow swath width and greatly reducing laser shadows from trees and buildings.

Quality GPS: Flights took place during optimal GPS conditions (e.g., 6 or more satellites and PDOP [Position Dilution of Precision] less than 3.0). Before each flight, the PDOP was determined for the survey day. During all flight times, a dual frequency DGPS base station recording at 1 second epochs was utilized and a maximum baseline length between the aircraft and the control points was less than 19 km (11.5 miles) at all times.

Ground Survey: Ground survey point accuracy (<1.5 cm RMSE) occurs during optimal PDOP ranges and targets a minimal baseline distance of 4 miles between GPS rover and base. Robust statistics are, in part, a function of sample size (n) and distribution. Ground survey points are distributed to the extent possible throughout multiple flight lines and across the survey area.

50% Side-Lap (100% Overlap): Overlapping areas are optimized for relative accuracy testing. Laser shadowing is minimized to help increase target acquisition from multiple scan angles. Ideally, with a 50% side-lap, the nadir portion of one flight line coincides with the swath edge portion of overlapping flight lines. A minimum of 50% side-lap with terrain-followed acquisition prevents data gaps.

Opposing Flight Lines: All overlapping flight lines are opposing. Pitch, roll and heading errors are amplified by a factor of two relative to the adjacent flight line(s), making misalignments easier to detect and resolve.

LiDAR First Return Point Density

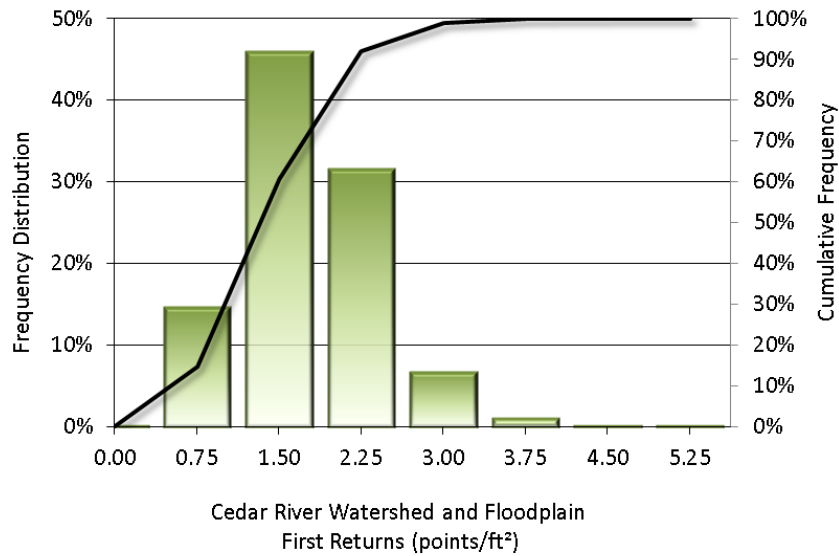


Figure 14: Frequency distribution of first return densities of the 30 x 30 m gridded study area

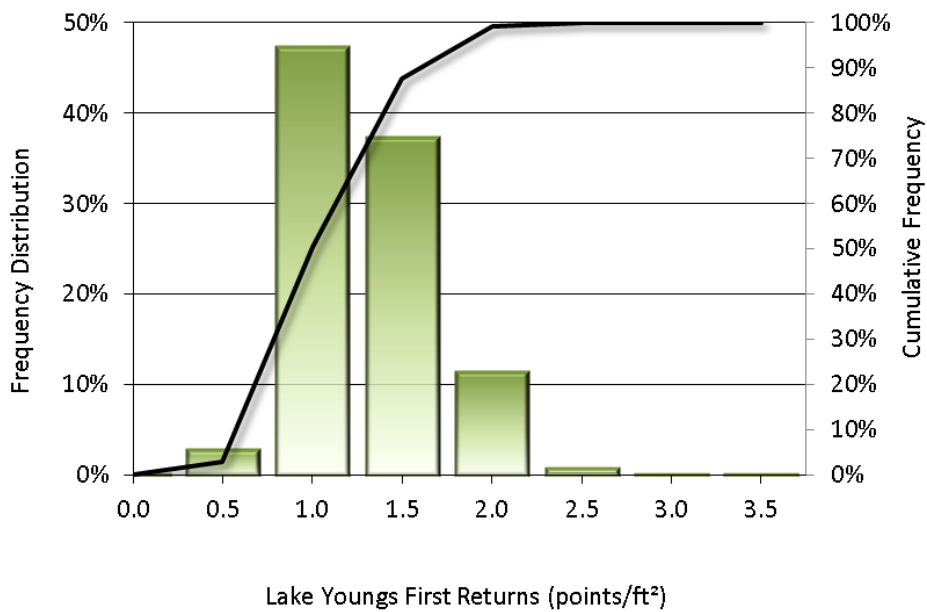


Figure 15: Frequency distribution of first return densities of the 30 x 30 m gridded study area

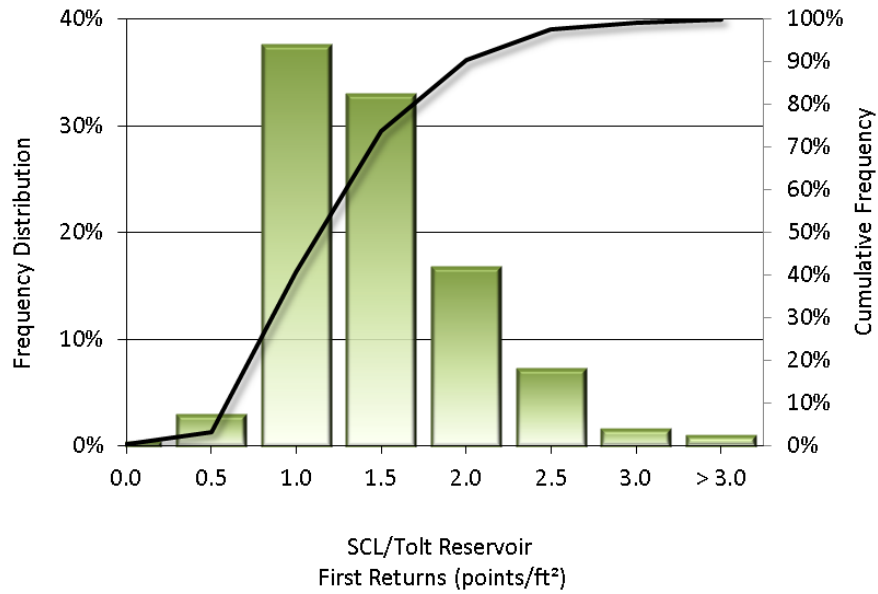


Figure 16: Frequency distribution of first return densities of the 30 x 30 m gridded study area

LiDAR Ground Point Density

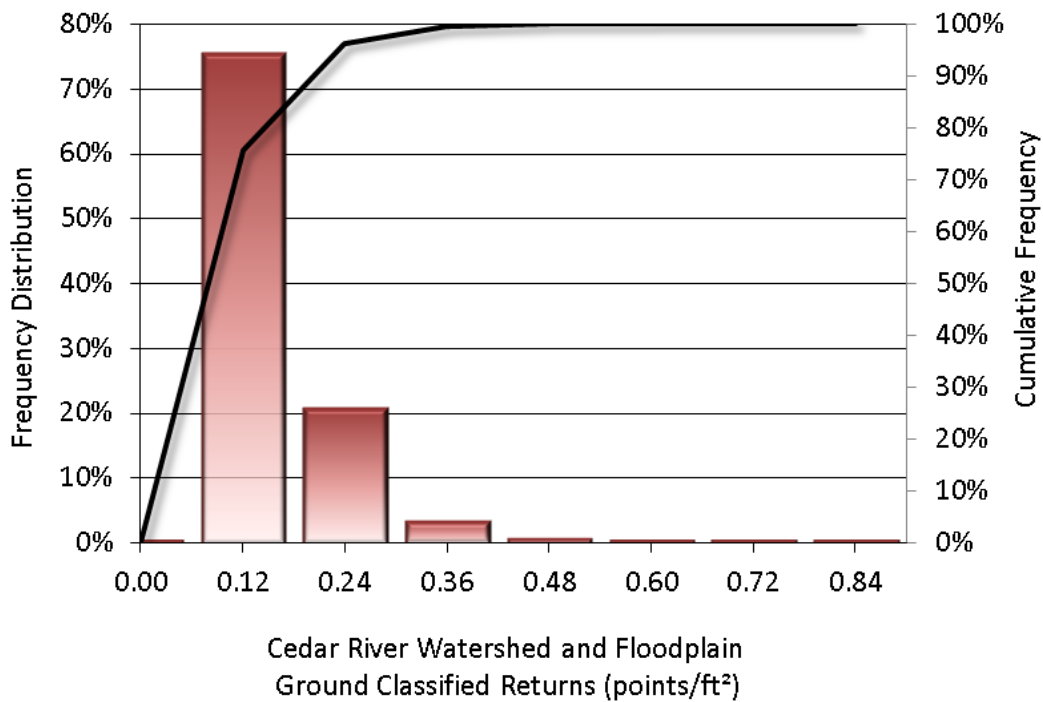


Figure 17: Frequency distribution of ground return densities of the 30 x 30 m gridded study area

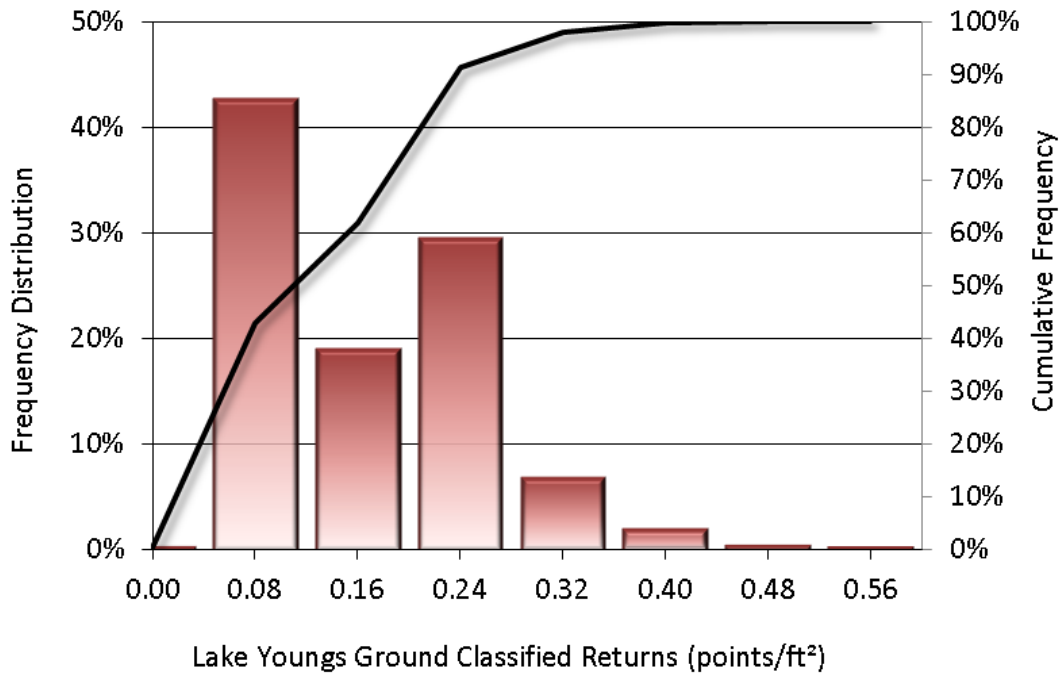


Figure 18: Frequency distribution of ground return densities of the 30 x 30 m gridded study area

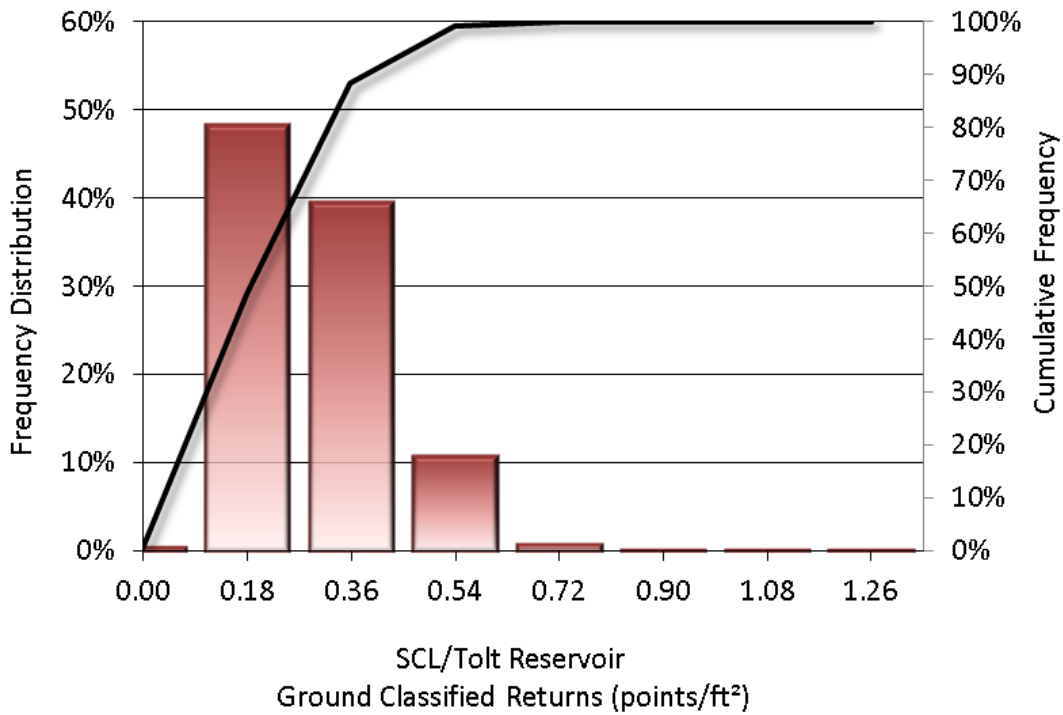


Figure 19: Frequency distribution of ground return densities of the 30 x 30 m gridded study area

LiDAR Absolute Accuracy

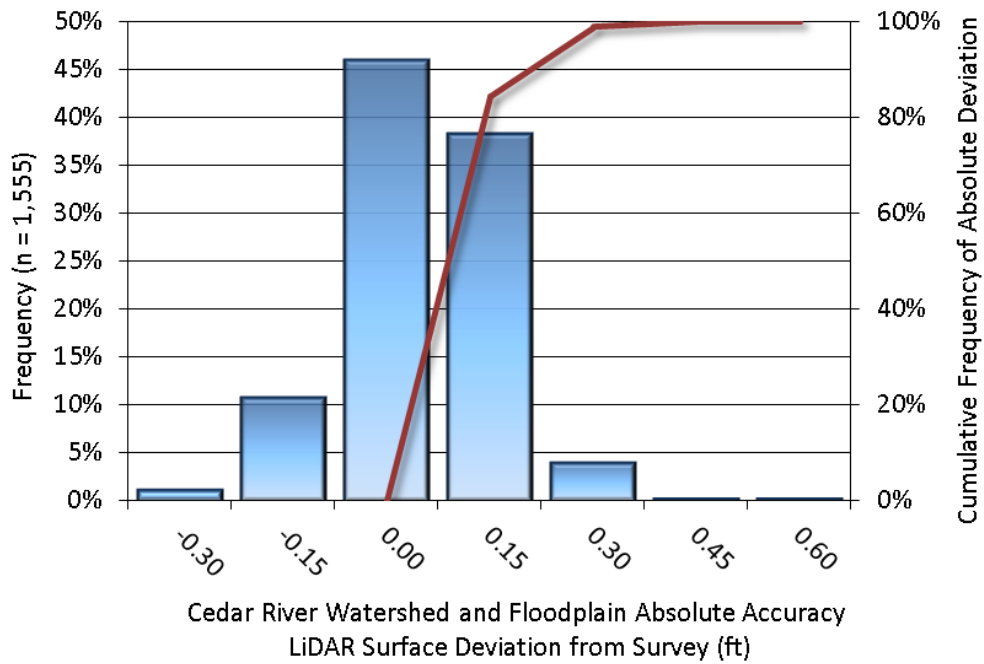


Figure 20: Frequency histogram for LiDAR surface deviation from ground survey point values in the Cedar River Watershed & Floodplain AOI

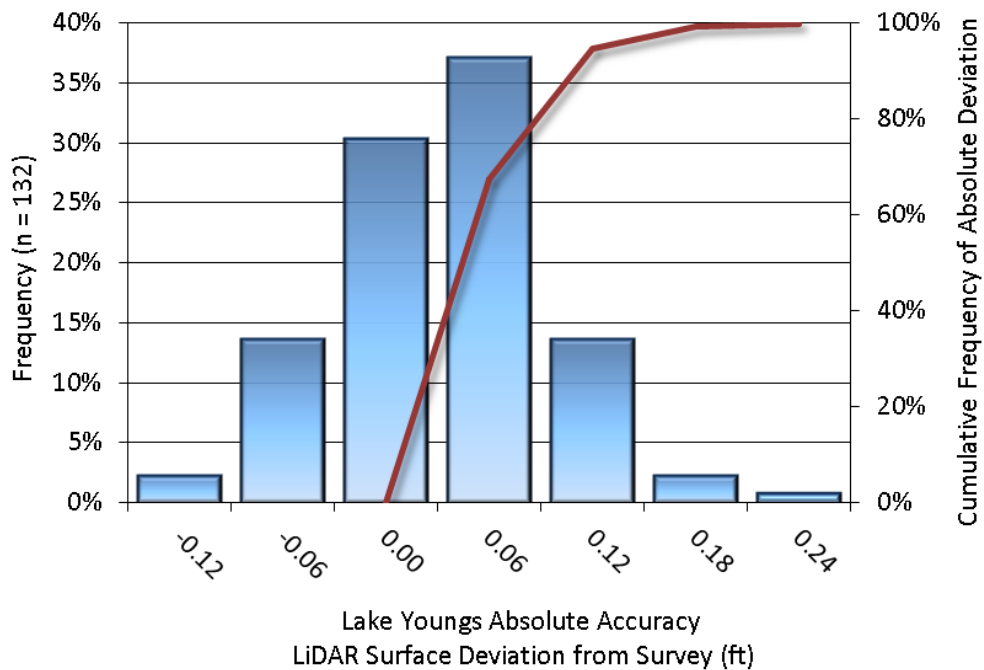


Figure 21: Frequency histogram for LiDAR surface deviation from ground survey point values in the Lake Youngs AOI

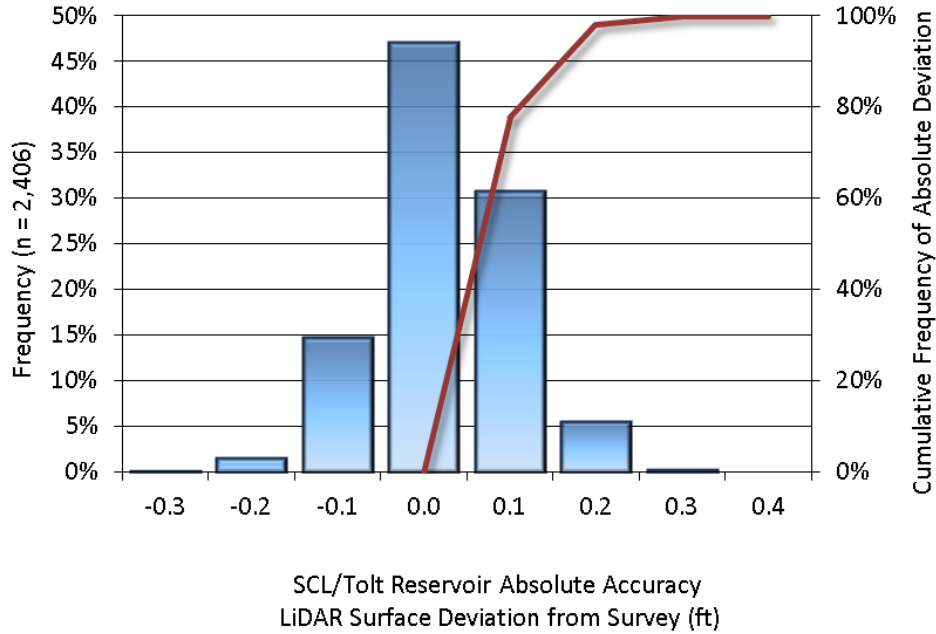


Figure 22: Frequency histogram for LiDAR surface deviation from ground survey point values in the SCL/Tolt Reservoir AOI

LiDAR Relative Accuracy

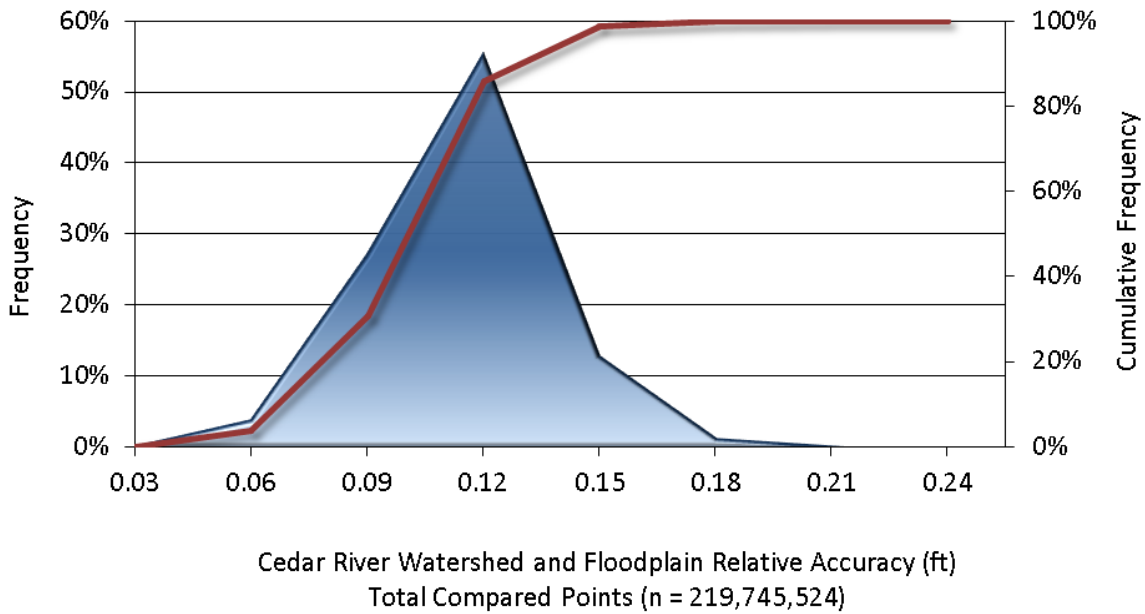


Figure 23: Frequency plot for relative vertical accuracy between flight lines in the Cedar River Watershed & Floodplain AOI

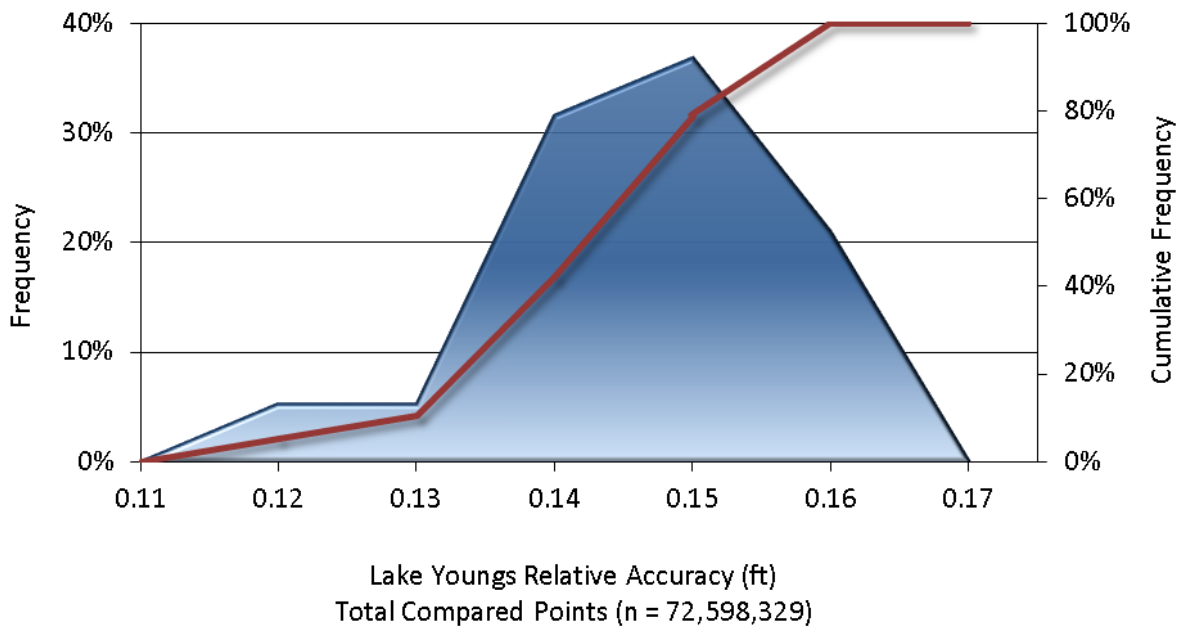


Figure 24: Frequency plot for relative vertical accuracy between flight lines in the Lake Youngs AOI

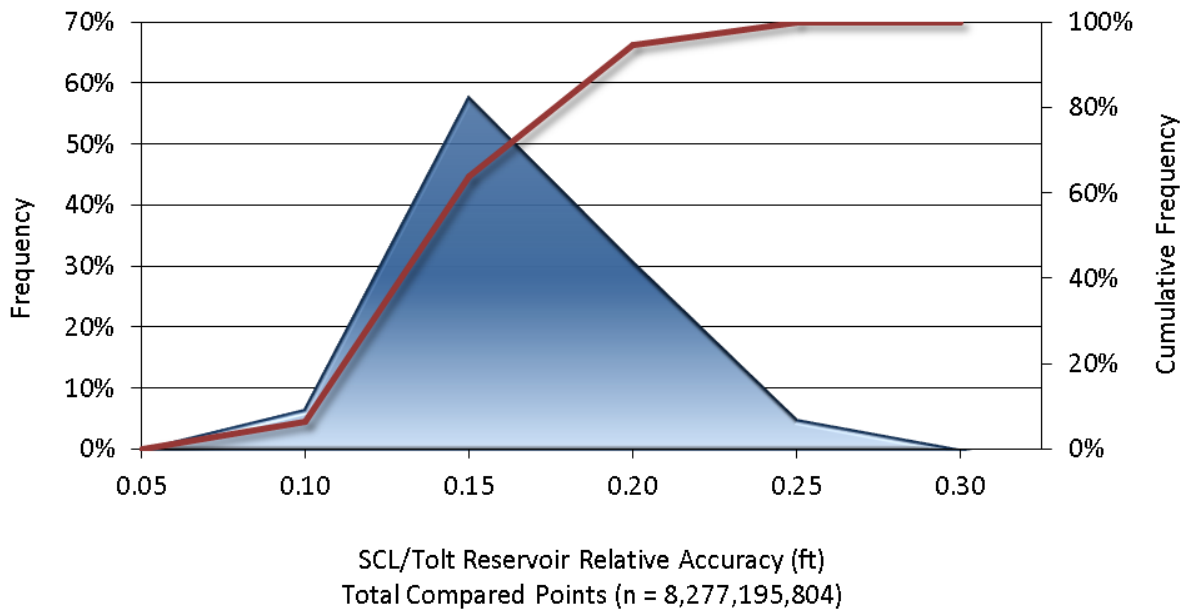


Figure 25: Frequency plot for relative vertical accuracy between flight lines in the SCL/Tolt Reservoir AOI